Synthesis of [59]Fullerenones through Peroxide-Mediated Stepwise Cleavage of Fullerene Skeleton Bonds and X-ray Structures of Their Water-Encapsulated Open-Cage Complexes

ARTICLE *in* JOURNAL OF THE AMERICAN CHEMICAL SOCIETY · JANUARY 2008

Impact Factor: 12.11 · DOI: 10.1021/ja0763798 · Source: PubMed

13 AUTHORS, INCLUDING:

Zuo Xiao
National Center for Nanoscience and Techno…
45 PUBLICATIONS **750** CITATIONS
SEE PROFILE

Zhenshan Jia
University of Nebraska at Omaha
20 PUBLICATIONS **230** CITATIONS
SEE PROFILE

J|A|C|S
ARTICLES
Published on Web 12/01/2007

Synthesis of [59]Fullerenones through Peroxide-Mediated Stepwise Cleavage of Fullerene Skeleton Bonds and X-ray Structures of Their Water-Encapsulated Open-Cage Complexes

Zuo Xiao,[†] Jiayao Yao,[†] Dazhi Yang,[†] Fudong Wang,[†] Shaohua Huang,[†] Liangbing Gan,*[,†,‡] Zhenshan Jia,[†] Zhongping Jiang,[†] Xiaobing Yang,[†] Bo Zheng,[†] Gu Yuan,[†] Shiwei Zhang,[†] and Zheming Wang*[,†]

Contribution from the Beijing National Laboratory for Molecular Sciences, Key Laboratory of Bioorganic Chemistry and Molecular Engineering of the Ministry of Education, College of Chemistry and Molecular Engineering, Peking University, Beijing 100871, and State Key Laboratory of Organometallic Chemistry, Shanghai Institute of Organic Chemistry, Chinese Academy of Sciences, 354 Fenglin Lu, Shanghai 200032, China

Received August 24, 2007; E-mail: gan@pku.edu.cn (L.G.); zmw@pku.edu.cn (Z.W.)

Abstract: Fullerene skeleton modification has been investigated through selective cleavage of the fullerene carbon−carbon bonds under mild conditions. Several cage-opened fullerene derivatives including three [59]fullerenones with an 18-membered-ring orifice and one [59]fullerenone with a 19-membered-ring orifice have been prepared starting from the fullerene mixed peroxide **1**, $C_{60}(OO^tBu)_6$. The prepositioned *tert*-butyl peroxy groups in **1** serve as excellent oxygen sources for formation of hydroxyl and carbonyl groups. The cage-opening reactions were initiated by photoinduced homolysis of the ^{t}Bu−O bond, followed by sequential ring expansion steps. A key step of the ring expansion reactions is the oxidation of adjacent fullerene hydroxyl and amino groups by diacetoxyliodobenzene (DIB). Aminolysis of a cage-opened fullerene derivative containing an anhydride moiety resulted in multiple bond cleavage in one step. A domino mechanism was proposed for this reaction. Decarboxylation led to elimination of one carbon atom from the C_{60} cage and formation of [59]fullerenones. The cage-opened [59]fullerenones were found to encapsulate water under mild conditions. All compounds were characterized by spectroscopic data. Single-crystal structures were also obtained for five skeleton-modified derivatives including two water-encapsulated fulleroids.

Introduction

Over the past 20 years, fullerene chemistry has been extensively studied.[1] The exohedral addition chemistry of fullerene, C_{60} in particular, has been well developed. Almost any functional group can be connected to the fullerene cage through a known reaction. Numerous fullerene derivatives have been prepared and investigated for their potential applications in material science[2] or in the pharmaceutical industry.[3] Compared to the rich exohedral addition chemistry, fullerene skeleton modification is still a young discipline. Skeleton modification requires controlled cleavage of fullerene carbon−carbon bonds. The process could produce many fascinating molecules. Consecutive cleavage of carbon−carbon bonds within a local region could open a large hole on the cage, through which atoms or small molecules may be inserted. Well-designed cleavage of multiple carbon−carbon bonds around the same carbon atom can replace the skeleton carbon atom to form heterofullerenes.[4] Analogous to the importance of heterocycles in organic chemistry, heterofullerenes have enormous potential in fullerene chemistry. Fullerene skeleton carbon atoms can also be eliminated to form norfullerenes by multiple fullerene bond cleavage.[5] A number of interesting fulleroids have been designed and studied by calculations such as bisazafullerene and azaborafullerene.[4,6] However, preparations of these compounds are difficult and have not been reported. Fullerene skeleton modi-

[†] Peking University.
[‡] Chinese Academy of Sciences.

(1) (a) Hirsch, A.; Brettreich, M. *Fullerenes: Chemistry and Reactions*; Wiley-VCH Verlag GmbH & Co. KGaA: Weinheim, Germany, 2005. (b) Thilgen, C.; Diederich, F. *Chem. Rev.* **2006**, *106*, 5049. (c) Martin, N. *Chem. Commun.* **2006**, 2093.
(2) (a) Prato, M. *Top. Curr. Chem.* **1999**, *199*, 173. (b) Wudl, F. *J. Mater. Chem.* **2002**, *12*, 1959. (c) Sawamura, M.; Kawai, K.; Matsuo, Y.; Kanie, K.; Kato, T.; Nakamura, E. *Nature* **2002**, *419*, 702. (d) Giacalone, F.; Martin, N. *Chem. Rev.* **2006**, *106*, 5136.
(3) (a) Friedman, S. H.; DeCamp, D. L; Sijbesma, R. P.; Srdanov, G.; Wudl, F.; Kenyon, G. L. *J. Am. Chem. Soc.* **1993**, *115*, 6506. (b) Toth, E.; Bolskar, R. D.; Borel, A.; Gonzalez, G.; Helm, L.; Merbach, A. E.; Sitharaman, B.; Wilson, L. J. *J. Am. Chem. Soc.* **2005**, *127*, 799. (c) Isobe, H.; Nakanishi, W.; Tomita, N.; Jinno, S.; Okayama, H.; Nakamura, E. *Chem.—Asian J.* **2006**, *1*, 167.
(4) (a) Rubin, Y. *Top. Curr. Chem.* **1999**, *199*, 67. (b) Hummelen, J. C.; Bellavia-Lund, C.; Wudl, F. *Top. Curr. Chem.* **1999**, *199*, 93. (c) Vostrowsky, O.; Hirsch, A. *Chem. Rev.* **2006**, *106*, 5191. (d) Hirsch, A. *Acc. Chem. Res.* **1999**, *32*, 795.
(5) (a) Powell, W. H.; Cozzi, F.; Moss, G. P.; Thilgen, C.; Hwu, R. J.-R.; Yerin, A. *Pure Appl. Chem.* **2002**, *74*, 629. (b) Troshin, P. A.; Avent, A. G.; Darwish, A. D.; Martsinovich, N.; Abdul-Sada, A. K.; Street, J. M.; Taylor, R. *Science* **2005**, *309*, 278.

fication remains an attractive yet also challenging frontier in fullerene chemistry.

In spite of the difficulty in modifying the fullerene skeleton, remarkable progress has been made. Wudl et al. reported the first open-cage derivative with a ketolactam moiety, which was used to make the first azafullerene, $C_{59}NR$.[7] Taylor et al. isolated a bislactone derivative from the air oxidation of $C_{70}Ph_8$.[8] Rubin et al. reported the synthesis of several open-cage derivatives including a bislactam derivative. The orifice in this compound is large enough to allow partial encapsulation of He or H_2. This is the first successful example of introducing an atom or molecule inside the fullerene cage through an orifice on the fullerene surface.[9] Komatsu et al. succeeded in making the hydrogen endohedral fullerene $H_2@C_{60}$ through a molecular surgery method. The work is a landmark in fullerene chemistry.[10] The largest opening on fullerene was produced by Iwamatsu's group, through which water or carbon monoxide can be inserted.[11] A number of related cage-opened fullerene derivatives have been reported recently by Orfanopoulos et al.[12]

We have reported the synthesis of fullerene mixed peroxides.[13] Further study indicates that the peroxy groups may be used to cleave fullerene C−C bonds selectively. Recently, we reported the oxidation of a fullerenediol into fullerene diketone with a ten-membered-ring orifice and the preparation of open-cage oxafulleroids embedded with furan and lactone moieties through Lewis acid-induced reactions of fullerene mixed peroxide.[14] Here we report the synthesis of [59]fulleroids with 18- and 19-membered-ring orifices by multistep chemical reactions starting from the fullerene hexaadduct $C_{60}(OO^tBu)_6$. These cage-opened fullerene derivatives are shown to be excellent molecular water traps and to form water-encapsulated complexes efficiently.

Results and Discussion

Strategies for Cleaving Fullerene Skeleton Bonds. Fullerene skeleton modification is a challenging task. Due to its unique spherical structure, selective cleavage of fullerene skeleton bonds requires strategies different from those in classic organic molecules. Current cage-opening methods usually employ two pathways: (1) formation of mono- or bisazafulleroids by insertion of a nitrogen atom into the 5,6-conjunction and subsequent ring expansion;[7,12] (2) formation of bisfulleroids initiated by [4 + 4] cycloaddition and subsequent ring enlargement.[9−12] Singlet oxygen is the most efficient reagent in ring expansion, which involves the formation of a dioxetane intermediate. Elemental sulfur, selenium, and amino aromatic compounds have also been used to expand the orifice effectively.[10−12]

Inspired by the singlet oxygen expansion process, we proposed the peroxide chemistry[15] based route as shown in Scheme 1. Fullerene is known to be an excellent radical scavenger.[16] Just like alkyl or aryl radicals, alkyl peroxy radicals add to C_{60} to form multiadducts through the cyclopentadienyl mode.[13] Selective cleavage of the R−O bond (path a), followed by intramolecular addition, could give the dioxetane species, which may then rearrange into the cage-opened diketone according to the same way as the singlet oxygen oxidation process.[7a] If the peroxy O−O bond is cleaved (path b), the epoxide will be formed. Ring-opening of the epoxide and oxidation of the resulting vicinal diol could also lead to the diketone.[14b]

Repeating the same cage-opening process within a local region on the fullerene surface could lead to the formation of large orifices and/or elimination of fullerene skeleton carbon atoms. For example, successive cleavage of three double bonds around the same pentagon could lead to an 18-membered orifice (Scheme 2). Steric hindrance is not a problem for such a

(6) (a) Karfunkel, H. R.; Dressler, T.; Hirsch, A. *J. Comput.−Aided Mol. Des.* **1992**, *6*, 521. (b) Jiao, H.; Chen, Z.; Hirsch, A.; Thiel, W. *Phys. Chem. Chem. Phys.* **2002**, *4*, 4916. (c) Xia, X.; Jelski, D. A.; Bowser, J. R.; George, T. F. *J. Am. Chem. Soc.* **1992**, *114*, 6493.

(7) (a) Hummelen, J. C.; Prato, M.; Wudl, F. *J. Am. Chem. Soc.* **1995**, *117*, 7003. (b) Hummelen, J. C.; Knight, B.; Pavlovich, J.; Gonzalez, R.; Wudl, F. *Science* **1995**, *269*, 1554.

(8) Birkett, P. R.; Avent, A. G.; Darwish, A. D.; Kroto, H. W.; Taylor, R.; Walton, D. R. M. *J. Chem. Soc., Chem. Commun.* **1995**, 1869.

(9) (a) Arce, M.-J.; Viado, A. L.; An, Y.-Z.; Khan, S. I.; Rubin, Y. *J. Am. Chem. Soc.* **1996**, *118*, 3775. (b) Rubin, Y. *Chem.−Eur. J.* **1997**, *3*, 1009. (c) Schick, G.; Jarrosson, T.; Rubin, Y. *Angew. Chem., Int. Ed.* **1999**, *38*, 2360. (d) Irle, S.; Rubin, Y.; Morokuma, K. *J. Phys. Chem. A* **2002**, *106*, 680. (e) Rubin, Y.; Jarrosson, T.; Wang, G.-W.; Bartberger, M. D.; Houk, K. N.; Schick, G.; Saunders, M.; Cross, R. J. *Angew. Chem., Int. Ed.* **2001**, *40*, 1543. (f) Nierengarten, J.-F. *Angew. Chem., Int. Ed.* **2001**, *40*, 2973. (g) Qian, W.; Bartberger, M. D.; Pastor, S. J.; Houk, K. N.; Wilkins, C. L.; Rubin, Y. *J. Am. Chem. Soc.* **2000**, *122*, 8333. (h) Qian, W.; Rubin, Y. *J. Org. Chem.* **2002**, *67*, 7683. (i) Qian, W.; Chuang, S.-C.; Amador, R. B.; Jarrosson, T.; Saunders, M.; Pieniazek, S.; Khan, S. I.; Rubin, Y. *J. Am. Chem. Soc.* **2003**, *125*, 2066.

(10) (a) Komatsu, K.; Murata, M.; Murata, Y. *Science* **2005**, *307*, 238. (b) Murata, Y.; Kato, N.; Komatsu, K. *J. Org. Chem.* **2001**, *66*, 7235. (c) Murata, Y.; Komatsu, K. *Chem. Lett.* **2001**, *30*, 896. (d) Murata, Y.; Murata, M.; Komatsu, K. *J. Org. Chem.* **2001**, *66*, 8187. (e) Murata, Y.; Murata, M.; Komatsu, K. *Chem.−Eur. J.* **2003**, *9*, 1600. (f) Murata, Y.; Murata, M.; Komatsu, K. *J. Am. Chem. Soc.* **2003**, *125*, 7152. (g) Sawa, H.; Wakabayashi, Y.; Murata, Y.; Murata, M.; Komatsu, K. *Angew. Chem., Int. Ed.* **2005**, *44*, 1981. (h) Murata, M.; Murata, Y.; Komatsu, K. *J. Am. Chem. Soc.* **2006**, *128*, 8024. (i) Chuang, S.-C.; Murata, Y.; Murata, M.; Mori, S.; Maeda, S.; Tanabea, F.; Komatsu, K. *J. Chem. Soc., Chem. Commun.* **2007**, 1278. (j) Chuang, S.-C.; Murata, Y.; Murata, M.; Komatsu, K. *J. Chem. Soc., Chem. Commun.* **2007**, 1751. (k) Chuang, S.-C.; Murata, Y.; Murata, M.; Komatsu, K. *J. Org. Chem.* **2007**, *72*, 6447.

(11) (a) Inoue, H.; Yamaguchi, H.; Iwamatsu, S.-i.; Uozaki, T.; Suzuki, T.; Akasaka, T.; Nagase, S.; Murata, S. *Tetrahedron Lett.* **2001**, *42*, 895. (b) Iwamatsu, S.-i.; Ono, F.; Murata, S. *J. Chem. Soc., Chem. Commun.* **2003**, 1268. (c) Iwamatsu, S.-i.; Ono, F.; Murata, S. *Chem. Lett.* **2003**, *32*, 614. (d) Iwamatsu, S.-i.; Uozaki, T.; Kobayashi, K.; Re, S.; Nagase, S.; Murata, S. *J. Am. Chem. Soc.* **2004**, *126*, 2668. (e) Iwamatsu, S.-i.; Murata, S. *Tetrahedron Lett.* **2004**, *45*, 6391. (f) Iwamatsu, S.-i.; Murata, S. *Synlett* **2005**, *14*, 2117. (g) Iwamatsu, S.-i.; Stanisky, C. M.; Cross, R. J.; Saunders, M.; Mizorogi, N.; Nagase, S.; Murata, S. *Angew. Chem., Int. Ed.* **2006**, *45*, 5337. (h) Inoue, H.; Yamaguchi, H.; Suzuki, T.; Akasaka, T.; Murata, S. *Synlett* **2000**, 1178. (i) Iwamatsu, S.-i.; Vijayalakshimi, P. S.; Hamajima, M.; Suresh, C. H.; Koga, N.; Suzuki, T.; Murata, S. *Org. Lett.* **2002**, *4*, 1217. (j) Suresh, C. H.; Vijayalakshimi, P. S.; Iwamatsu, S.-i.; Murata, S.; Koga, N. *J. Org. Chem.* **2003**, *68*, 3522.

(12) (a) Vougioukalakis, G. C.; Prassides, K.; Campanera, J. M.; Heggie, M. I.; Orfanopoulos, M. *J. Org. Chem.* **2004**, *69*, 4524. (b) Vougioukalakis, G. C.; Prassides, K.; Orfanopoulos, M. *Org. Lett.* **2004**, *6*, 1245. (c) Roubelakis, M. M.; Vougioukalakis, G. C.; Orfanopoulos, M. *J. Org. Chem.* **2007**, *72*, 6526. (d) Roubelakis, M. M.; Murata, Y.; Komatsu, K.; Orfanopoulos, M. *J. Org. Chem.* **2007**, *72*, 7042.

(13) (a) Gan, L. B.; Huang, S. H.; Zhang, X.; Zhang, A. X.; Cheng, B. C.; Cheng, H.; Li, X. L.; Shang, G. *J. Am. Chem. Soc.* **2002**, *124*, 13384. (b) Xiao, Z.; Wang, F. D.; Huang, S. H.; Gan, L. B.; Zhou, J.; Yuan, G.; Lu, M. J.; Pan, J. Q. *J. Org. Chem.* **2005**, *70*, 2060. (c) Gan, L. B. *Pure Appl. Chem.* **2006**, *78*, 841. (d) Gan, L. B. *C. R. Chim.* **2006**, *9*, 1001.

(14) (a) Huang, S. H.; Xiao, Z.; Wang, F. D.; Zhou, J.; Yuan, G.; Zhang, S. W.; Chen, Z. F.; Thiel, W.; Schleyer, P. R.; Zhang, X.; Hu, X. Q.; Chen, B. C.; Gan, L. B. *Chem.−Eur. J.* **2005**, *11*, 5449. (b) Huang, S. H.; Wang, F. D.; Gan, L. B.; Yuan, G.; Zhou, J.; Zhang, S. W. *Org. Lett.* **2006**, *8*, 277. (c) Wang, F. D.; Xiao, Z.; Gan, L. B.; Jia, Z. S.; Jiang, Z. P.; Zhang, S. W.; Zheng, B.; Gu, Y. *Org. Lett.* **2007**, *9*, 1741.

(15) (a) Swern, D., Ed. *Organic Peroxides*; Wiley-Interscience: New York, 1971. (b) Koenig, T. In *Free Radicals I*; Kochi, J. K., Ed.; Wiely-Interscience: New York, 1973. (c) Patai, S., Ed. *The Chemistry of Organic Peroxides*; Wiley-Interscience: New York, 1983. (d) Lane, B. S.; Burgess, K. *Chem. Rev.* **2003**, *103*, 2457.

(16) (a) Taylor, R. *Lecture Notes on Fullerene Chemistry*; Imperial College Press: London, 1999; p 91. (b) Krusic, P. J.; Wasserman, E.; Keizer, P. N.; Morton, J. R.; Preston, K. F. *Science* **1991**, *254*, 1183. (c) Borghi, R.; Lunazzi, L.; Placucci, G.; Cerioni, G.; Plumitallo, A. *J. Org. Chem.* **1996**, *61*, 3327. (d) Troyanov, S. I.; Troshin, P. A.; Boltalina, O. V.; Ioffe, I. N.; Sidorov, L. N.; Kemnitz, E. *Angew. Chem., Int. Ed.* **2001**, *40*, 2285. (e) Troyanov, S. I.; Shustova, N. B.; Popov, A. A.; Sidorov, L. N.; Kemnitz, E. *Angew. Chem., Int. Ed.* **2005**, *44*, 432. (f) Shustova, N. B.; Newell, B. S.; Miller, S. M.; Anderson, O. P.; Bolskar, R. D.; Seppelt, K.; Popov, A. A.; Boltalina, O. V.; Strauss, S. H. *Angew. Chem., Int. Ed.* **2007**, *46*, 4111.

Scheme 1

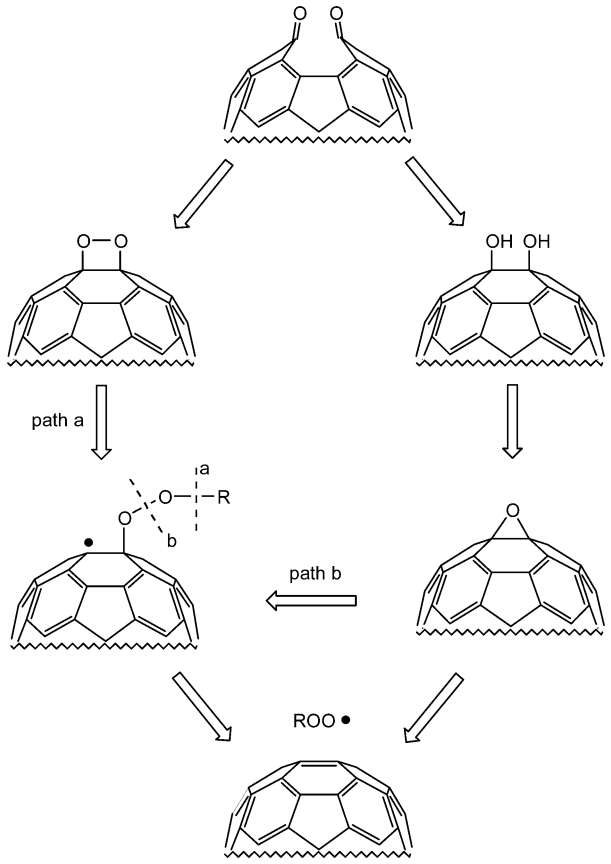

Scheme 2

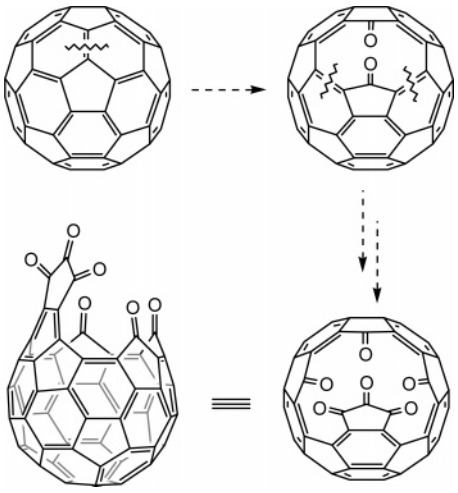

compound since the pentagon would be lifted up from the cage surface just like a half-opened cap. Controlling the chemo- and regioselectivity is the key point for this approach.

Cage-Opening through Photolysis of $C_{60}(OO^tBu)_6$. The hexaadduct **1** was prepared according to the improved procedure we reported recently.[17] It decomposes slowly if exposed to visible light. We have previously reported that luminescent light bulb irradiation of **1** in the presence of excess iodine gave an open-cage diketone fullerene derivative.[18] The reaction needed

Scheme 3

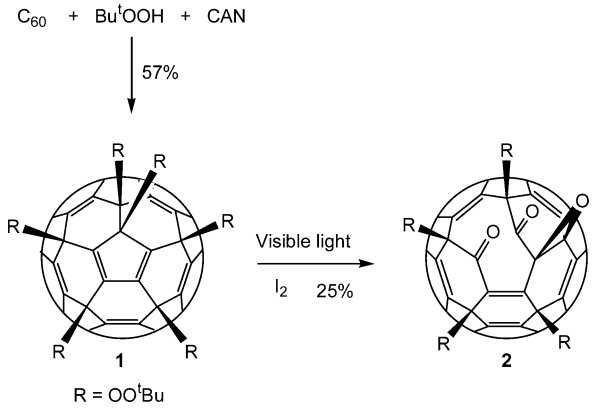

40 h under the previously reported conditions. We have now optimized the condition by using an LED blue lamp (dominant wavelength at 470 nm) as the light source. In this case, just 1 equiv of iodine was needed and the reaction time was reduced to 1.5 h on a scale of 2.9 g of **1**. The yield of **2** is still the same as previously reported at 25% (Scheme 3).

We have previously assigned the structure of compound **2** as the regioisomer **2a** on the basis of spectroscopic data.[18] The MS and NMR spectra revealed the right functional groups on

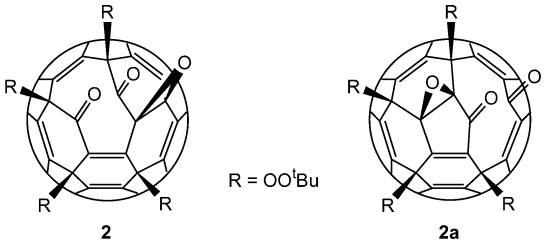

the compound, but they could not differentiate the two isomers **2** and **2a** because both structures are C_1 symmetric. In our previous assignment, we favored **2a** on the basis of the fact that the strong C═O stretching band of **2** at 1748 cm^{-1} is close to that of cyclopentanone (1743 cm^{-1}) instead of cyclohexanone (1715 cm^{-1}). However, this assignment is incorrect according to the X-ray structure of **4l′** (Figure 1), which was prepared from **2** (see sections below). Apparently the unique fullerene spherical structure caused the shift of the IR stretching band. The correct structure for the photolysis reaction should be **2** rather than **2a**.

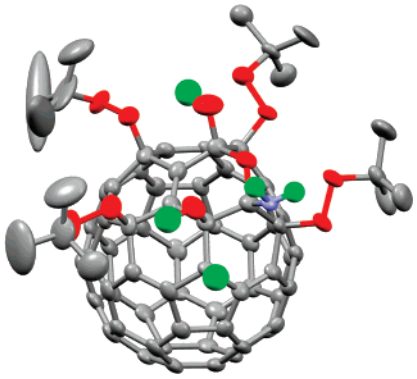

Figure 1. X-ray structure of compound **4l′**. Ellipsoids were drawn at the 50% level. For clarity hydrogen atoms of the *tert*-butyl groups are not shown. Key: gray, carbon; red, oxygen; blue, nitrogen; green, hydrogen.

(17) Wang, F. D.; Xiao, Z.; Yao, Z. P.; Jia, Z. S.; Huang, S. H.; Gan, L. B.; Zhou, J.; Yuan, G.; Zhang, S. W. *J. Org. Chem.* **2006**, *71*, 4374.
(18) Huang, S. H.; Xiao, Z.; Wang, F. D.; Gan, L. B.; Zhang, X.; Hu, X. Q.; Zhang, S. W.; Lu, M. J.; Pan, J. Q.; Xu, L. *J. Org. Chem.* **2004**, *69*, 2442.

Scheme 4

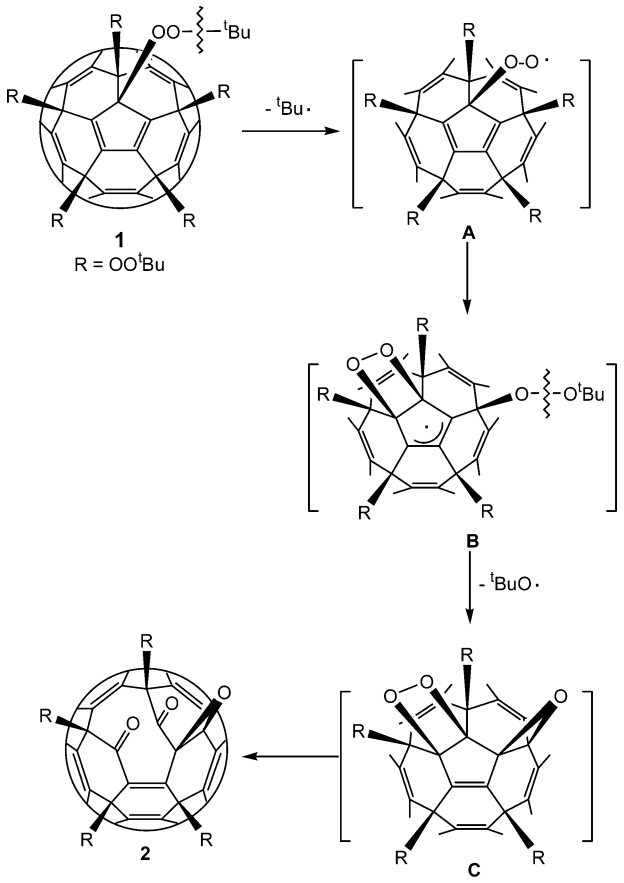

Scheme 5

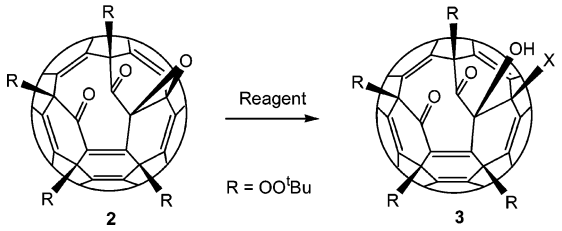

Scheme 4 shows a revised reaction pathway for the photochemical reaction leading to compound **2**. The first step is the homolytic cleavage of the O−^{t}Bu bond on the central pentagon to give the fullerene peroxide radical **A**. Then intramolecular radical addition of **A** forms intermediate **B** with a 1,2-dioxetane and an allyl radical moiety. Loss of one *tert*-butoxy radical from **B** leads to intermediate **C**. Finally, rearrangement of the 1,2-dioxetane moiety in intermediate **C** results in the cage-opened compound **2**. Other peroxy bonds may be cleaved as well under the photolysis conditions, which explains the low yield of **2**. Addition of iodine is essential. Without iodine the photolysis reaction only gave inseparable complex mixtures. One possible role of the added iodine is trapping the radical byproducts such as *tert*-butyl radical, thus preventing them from reacting with **2**.

Epoxide Ring-Opening Reaction for Compound 2. The epoxy moiety in compound **2** is a good starting point for further orifice expansion reaction. We tried various ways to open the epoxy moiety (Scheme 5). When Lewis acids $FeCl_3$ and $FeBr_3$ were used, the corresponding halohydrins **3b** and **3c** were obtained (Table 1) in good yield. Treating **2** with PPh_3 and I_2 gave the iodohydrin **3d**.[19] The good regioselectivity of these epoxide-opening reactions is in agreement with the cationic mechanism in the first step. The two cations resulting from the epoxy O−C bond cleavage have different stabilities. The cation next to an electron-withdrawing carbonyl group is less stable. Triphenylphosphine could reduce the bromide **3c** into the hydride **3e**. Boron trifluoride gave a mixture of products. Only the boron Lewis acid $B(C_6F_5)_3$ gave the desired vicinal diol **3a**.

Table 1

	X	reagent	yield (%)
3a	OH	$B(C_6F_5)_3$	60
3b	Cl	$FeCl_3$	84
3c	Br	$FeBr_3$	81
3d	I	$PPh_3 + I_2$	58
3e	H	(1) $FeBr_3$, (2) PPh_3	57

The products were characterized by ESI-MS, NMR, and IR spectra. ESI-MS spectra of these compounds all gave clear molecular ion peak as the base peak. Relative locations of the addends resulting from the epoxy-opening were confirmed by HMBC spectra. The HMBC spectra of the vicinal diol **3a** showed clear correlation signals for the two sp^3 fullerene carbons at 82.78 and 80.68 ppm and the two hydroxyl groups at 6.28 and 4.88 ppm, indicating the vicinal diol moiety. The HMBC spectrum of the chlorohydrin **3b** showed a correlation signal between the carbonyl carbon at 196.9 ppm and the OH proton at 5.93 ppm, indicating the OH group is adjacent to the carbonyl group.

^{13}C NMR chemical shifts of the carbonyl groups are almost the same for the epoxy-opened derivatives **3** and the epoxide **2**, which appear at 198 and 194 ppm, varying within a 2 ppm range. However, the absorption band of the C═O stretching in the IR spectrum shows a significant decrease, from 1748 cm^{-1} for **2** to 1731−1744 cm^{-1} for compounds **3**. The C═O stretching bands of **3** are now closer to that of cyclohexanone (1715 cm^{-1}). Therefore, the strain of the epoxy moiety in **2** is a major source of the increase of its C═O stretching bands.

Protection of the Diketone by Formation of Aminoketal. Oxidation of the vicinal diol moiety in **3a** was then tested under various conditions, but all attempts were unsuccessful. Only complex mixtures were observed. The diketone moiety probably interfered with the oxidation. Therefore, to avoid its interference, we then tried to protect the diketone by converting it to ketal (Scheme 6). We have reported previously that the adjacent fullerenedione could be coupled by oxygen nucleophiles in the presence of a catalytic Lewis acid to form ketal/hemiketal derivatives.[14b] However, a similar reaction was unsuccessful for compounds **3**. Upon changing the oxygen nucleophiles to nitrogen nucleophiles, the aminoketal/hemiketal derivatives **4** were obtained in good yields (Scheme 6).

The amine coupling reactions are quite sensitive to steric hindrance. The reaction of NH_3(g) took only a few seconds at room temperature to convert all diketone to the products. For aromatic amines, it usually took several hours even at higher temperature. The regioselectivity also depends on the steric factor. Bulky amines only form the less crowded isomer **4**.

(19) Huang, S. H.; Yang, X. B.; Zhang, X.; Hu, X. Q.; Gan, L. B.; Zhang, S. W. *Synlett* **2006**, *8*, 1266.

Scheme 6

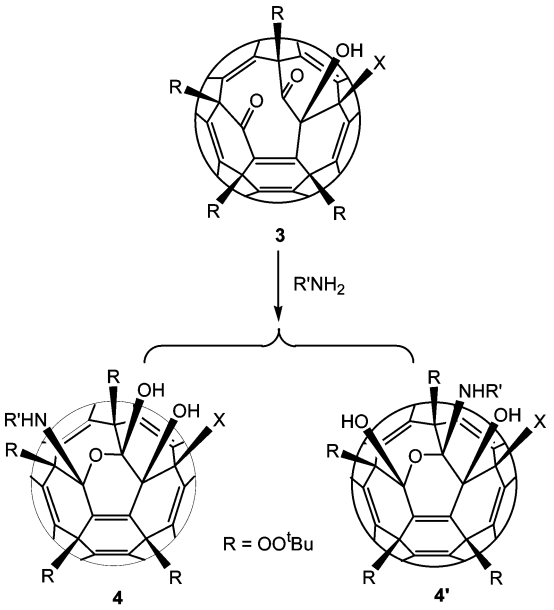

X	R'	4		yield %	4'	
OH	Ph	85	**4a**	-		
OH	*p*-MeOC$_6$H$_4$	85	**4b**	-		
OH	*p*-BrC$_6$H$_4$	79	**4c**	-		
OH	*p*-TsNH	74	**4d**	-		
OH	H	43	**4e**	43	**4e'**	
OH	(MeO)$_2$CHCH$_2$	78	**4f**	-		
Cl	*p*-MeOC$_6$H$_4$	65	**4g**	-		
Cl	(MeO)$_2$CHCH$_2$	85	**4h**	-		
Cl	H	18	**4i**	64	**4i'**	
H	(MeO)$_2$CHCH$_2$	81	**4j**	-		
H	(EtO)$_2$CHCH$_2$	89	**4k**	-		
H	H	27	**4l**	67	**4l'**	

Ammonia forms both regioisomers **4** and **4′**. The yield of **4′** is even higher than that of **4**, indicating the carbonyl adjacent to the isolated fullerene C═C double bond in the center is more electron rich due to partial conjugation.

Formation of the aminoketal/hemiketal was confirmed by spectroscopic data. In the ^{13}C NMR spectra of compounds **4**, there is no signal for the carbonyl group, and two strong sp^3 signals appear in the range from 100 to 90 ppm corresponding to the two aminoketal/hemiketal carbons. In the IR spectra, the strong C═O stretching band of the precursor **3** disappeared as expected. The two regioisomers of the NH_3 derivatives **4** and **4′** have very similar spectral data. It is impossible to differentiate the two. Fortunately, we got the single crystal of the more polar **4l′** by slow evaporation of its CS_2, toluene, and ethanol (1:1:1) solution at 5 °C. The X-ray crystallography of **4l′** showed clearly that the NH_3 group is added to the isolated carbonyl group not the conjugated carbonyl group (Figure 1). The locations of the vicinal hydroxyl and hydride groups are consistent with our earlier HMBC analysis of compounds **3a**−**e**.

The X-ray structure of **4l′** also serves as the key evidence for assigning the structure of its precursor as **2** instead of **2a**. It is impossible for structure **2a** to produce **4l′** under the present epoxide-opening and subsequent amination conditions (Scheme 7). Therefore, it was a mistake for us to propose the **2a** structure in 2004.[18]

Cage-Opening through Hypervalent Iodine Oxidation. After the protection of the diketone, we then tried the oxidation

Scheme 7

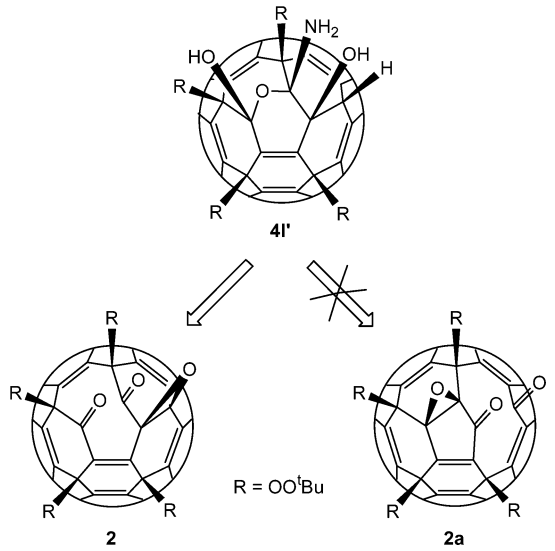

Scheme 8

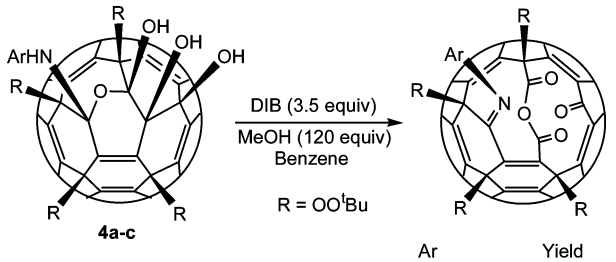

	Ar	Yield
5a	Ph	60%
5b	p-MeOC$_6$H$_4$	50%
5c	p-BrC$_6$H$_4$	59%

of the vicinal diol again. Similar to our previous result, diacetoxyliodobenzene (DIB) is the best oxidant for this oxidation reaction.[14b] Arylamine derivatives **4a**−**c** reacted with excess DIB (3.5 equiv) smoothly to give the cage-opened product **5** (Scheme 8). Some methanol (120 equiv) was added to speed the reaction and also to improve the yield. In the oxidation process the three hydroxyl groups in **4** were oxidized into three carbonyl groups, one in the ketone and two in the anhydride bridge. The amino group was also oxidized into the imino group. Ammonia and primary amine derivatives **4d**−**f** gave complex mixtures under various oxidation conditions.

The above oxidation process results in the loss of four protons. This is clearly shown in their ESI-MS spectra. The molecular ion peaks of **5a**, **5b**, and **5c** appear at *m*/*z* 1261, 1231, and 1311, respectively, all 4 units lower compared to those of their precursors **4a** (*m*/*z* 1265), **4b** (*m*/*z* 1235), and **4c** (*m*/*z* 1315). The IR spectra of compounds **5** show a strong peak at 1860 ± 1 cm^{-1} and a weak peak at 1800 ± 1 cm^{-1} which are characteristic of an anhydride group. The ketone group appears at 1746 ± 1 cm^{-1}. The ^{1}H and ^{13}C NMR spectra are also in agreement with the proposed structure.

A possible mechanism of this reaction is shown in Scheme 9. The amino group is the most reactive site. The first DIB molecule converts the amino group into an imino group and opens the aminoketal into an oxonium intermediate, **D**. Rearrangement of the oxonium **D** forms the carbocation **E**. Loss of a proton from **E** forms intermediate **F**. Finally, another DIB molecule oxidizes the vicinal diol moiety of intermediate **F** into two carbonyl groups.

Scheme 9

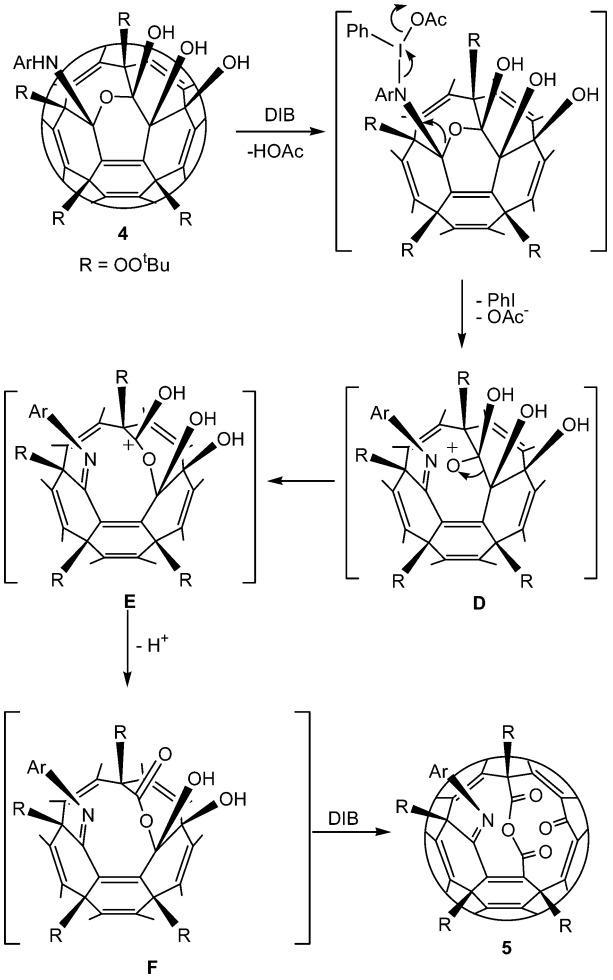

Scheme 10

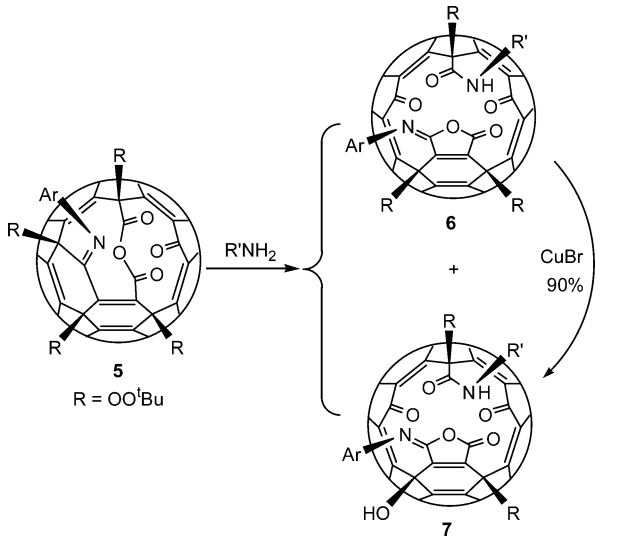

Table 2

amino group					
Ar	R′		yield (%)		yield (%)
4-MeOC$_6$H$_4$	4-MeOC$_6$H$_4$	**6a**	34	**7a**	15
Ph	Ph	**6b**	21	**7b**	19
Ph	4-MeOC$_6$H$_4$	**6c**	30	**7c**	24
4-BrC$_6$H$_4$	4-MeOC$_6$H$_4$	**6d**	23	**7d**	24
Ph	NH_2	**6e**	30	**7e**	30
Ph	H	**6f**	30	**7f**	31

The reaction was monitored by the TLC method. We observed that some polar intermediates appeared in the reaction, but these polar intermediates were too unstable to be isolated. They were probably the intermediates in the proposed mechanism. The addition of methanol may offer a more polar environment, thus stabilizing these intermediates and speeding the multistep oxidation process.

Orifice Expansion by Intramolecular Domino Rearrangement Initiated by Amino Reagents. Compared with the cage-opened diketone **2**, compounds **5** have two holes on the fullerene surface separated by an anhydride bridge. To expand the orifice, we tried to open the anhydride bridge and fuse the two orifices into one large orifice. Oxygen nucleophiles such as water and methanol are too weak to react with the anhydride carbonyls even in the presence of Lewis acids. Primary amines reacted with the anhydride efficiently to give two products, **6** and **7** (Scheme 10). Compounds **6** and **7** are essentially the same except that compound **6** has three *tert*-butyl peroxy groups whereas compound **7** has two *tert*-butyl peroxy groups and one hydroxyl group. Treating **6** with CuBr gave **7** in 90% yield. Both **6** and **7** have an 18-membered-ring orifice on the fullerene cage.

The spectroscopic data of **6** and **7** are in agreement with the structures depicted in Scheme 10. For example, the amide proton of **6a** showed a characteristic signal at 8.93 ppm in the ^{1}H NMR spectra. The ^{13}C NMR spectrum of **6a** shows two carbonyl signals at 185.56 and 184.20 ppm. The amide and lactone carbonyl signals appear at 160.97 and 162.52 ppm, respectively. In the IR spectrum, the anhydride C═O stretching bands of **5** at 1860 cm^{-1} disappeared in **6a**. Instead, **6a** showed strong absorption bands at 1802, 1748, and 1699 cm^{-1} attributable to the lactone, ketone, and amide carbonyl stretching bands, respectively.

The spectroscopic data indicate what groups are present in compounds **6** and **7** conclusively, but there are many possibilities to arrange these groups. It is not possible to assign the exact structure on the basis of these spectroscopic data. X-ray single-crystal analysis must be performed to solve the problem. To grow suitable crystals for X-ray analysis, we prepared various analogues as shown in Table 2 and tried different conditions of crystallization. A red crystal of **6a** was obtained by slow evaporation of its solution in CS_2/$CHCl_3$/CH_3OH (1:3:1) at 5 °C.

The X-ray structure of **6a** is shown in Figure 2. One of the carbon atoms at the original pentagon is separated from the pentagon and forms the amide moiety. The original pentagon in the center is converted into an isomaleimide moiety and completely lifted up from the cage surface.

A novel intramolecular domino rearrangement reaction pathway is proposed in Scheme 11. In the first step, the amino nucleophile attacks the more electron deficient carbonyl of the anhydride bridge and cleaves the bridge to form the amide and carboxylic acid groups of intermediate **G**. The carboxylic acid group does not react with the amide to form imide. Instead, it adds to the imino group to form the amino lactone intermediate **H**. This amino group of intermediate **H** is next to a *tert*-butyl peroxy group. The proton of the amino group readily forms a H-bond with the peroxy oxygen atom, resulting in formation

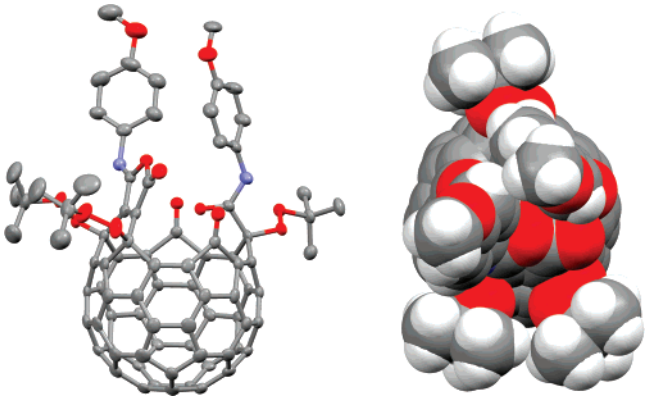

Figure 2. X-ray structure of compound **6a**. Ellipsoids were drawn at the 50% level. For clarity hydrogen atoms of the plot on the left are not shown. Key: gray, carbon; red, oxygen; blue, nitrogen; white, hydrogen.

Scheme 11

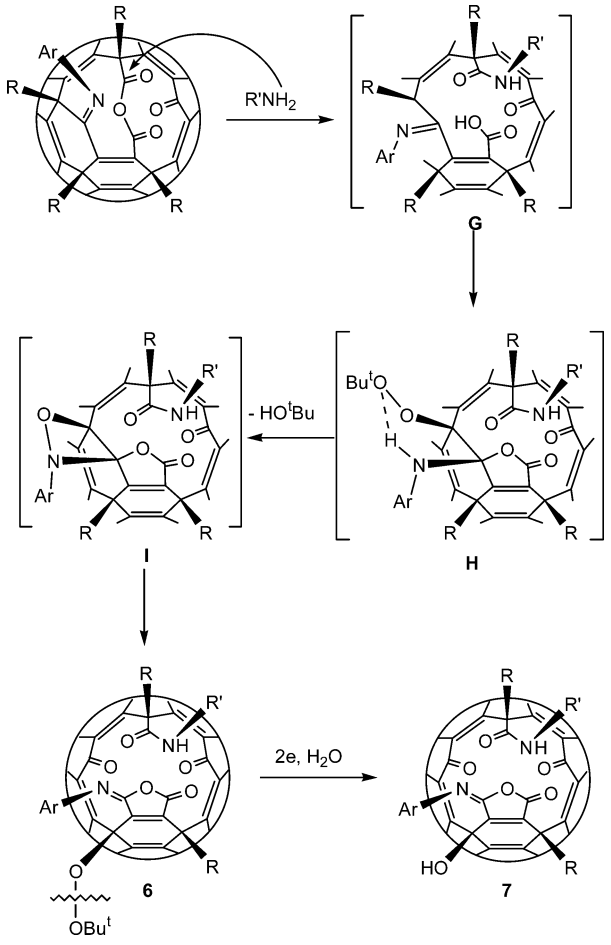

of a six-membered-ring transition state. Loss of *tert*-butyl alcohol from **H** gives intermediate **I** with an unstable oxazetidine moiety, which rearranges into a ketone and an imino group to form the final open-cage derivative **6**. The driving force of the last step may be due to the strain-releasing effect. The X-ray structure of **6a** indicates that the isomaleimide ring is planar.

Formation of the hydroxyl product **7** is probably due to reduction of the *tert*-butyl peroxy group by excess amines in the system. This is supported by the fact that a prolonged reaction time could give more **7** and less **6** and also the fact that **6** could be reduced to **7** by CuBr (Scheme 10). The coordination of both the oxygen on the *tert*-butyl peroxy group

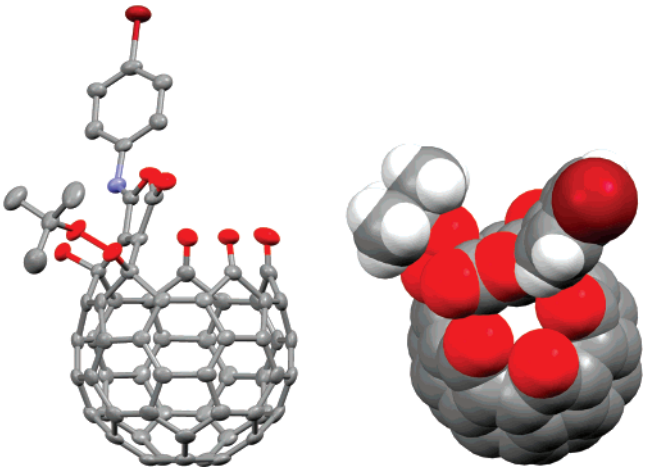

Figure 3. X-ray structure of compound **13**. Ellipsoids were drawn at the 50% level. For clarity hydrogen atoms of the plot on the left and carbon atoms behind the orifice of the CPK model are not shown. Key: gray, carbon; red, oxygen; blue, nitrogen; white, hydrogen; dark red, bromine.

Scheme 12

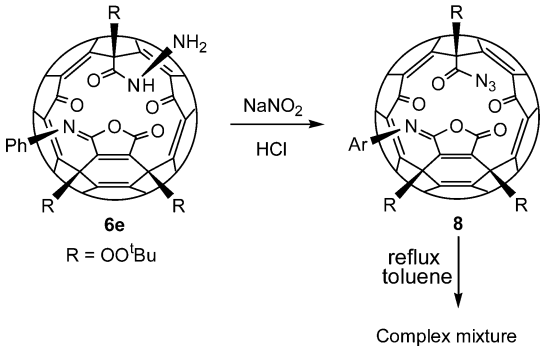

and the imino nitrogen with CuBr may be responsible for the high chemoselective reduction. The location of the hydroxyl group in **7** could not be assigned by spectroscopic data. The X-ray structure shown in Figure 3 provides conclusive evidence (see the next section).

Formation of [59]Fullerenones. Even though a large orifice is present in compounds **6** and **7**, the opening is completely blocked by the amide group as can be seen from the space-filling model in Figure 2. To remove the orifice-blocking amide, we tried several methods starting from different amino analogues. The arylamides are too stable to be hydrolyzed under normal conditions. The hydrazine derivative **6e** could react with $NaNO_2$ and HCl to form the azide derivative **8**, but the expected Curtis rearrangement did not occur; instead slow decomposition was observed when **8** was refluxed in toluene (Scheme 12).

Then we tried the reaction of **6e** and **7e** with Br_2 in an effort to prepare acyl bromide, which should be easier to hydrolyze into carboxylic acid. The reaction was very fast with excess Br_2. Products **9** and **10** were isolated from the reaction of **6e** and **7e**, respectively (Scheme 13). The bromination products **9** and **10** could be reduced back to **6e** and **7e** by excess $Na_2S_2O_3$ quantitatively. This indicates that the hydrazinocarbonyl moiety has been transformed to a bromoazocarbonyl moiety instead of the acyl bromide, which could not be reduced back to **6e** or **7e**. Similar bromination reactions have been reported before for other hydrazine compounds without a fullerene group.[20] The azo moiety in **9** and **10** could exist as both *E* and *Z* isomers. In the case of **10**, both isomers were isolated (see the Supporting

Scheme 13

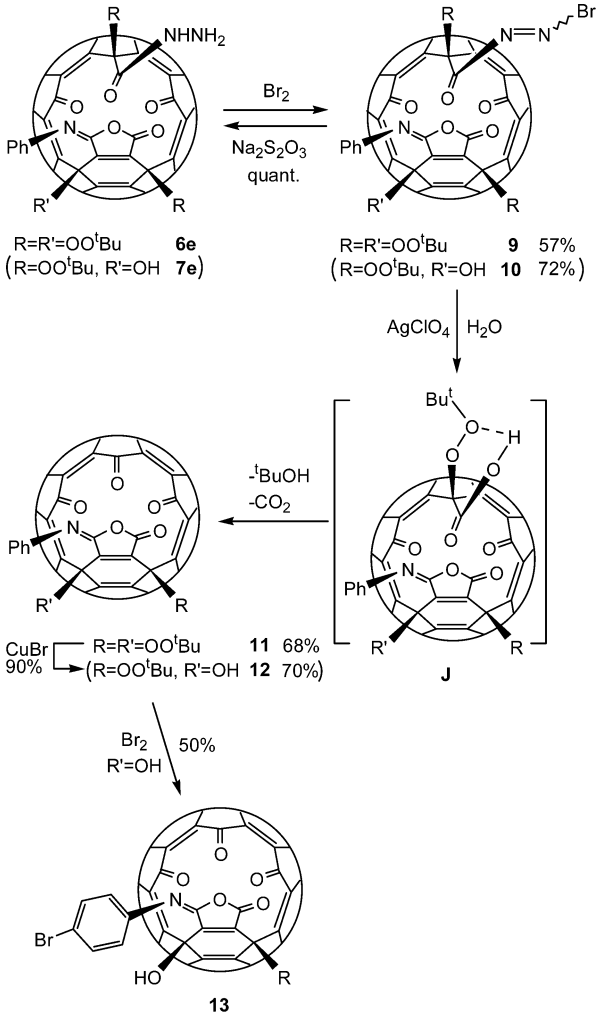

Information). However, it is not possible to assign the stereochemistry of the azo group at present.

Further treatment of the azo derivatives **9** and **10** with $AgClO_4$ eliminated the acyl group successfully. During the reaction a highly polar species was observed by TLC. It is probably the carboxylic acid derivative **J**. However, it was not stable and decomposed into the less polar products **11** and **12**, respectively, upon silica gel column chromatography. The decarboxylation may proceed via the six-membered transition state shown in Scheme 13.

NMR, ESI-MS, and IR spectra all suggest elimination of the amide carbon and formation of the C_{59} triketone **11** and **12**. To grow crystals, we treated **12** with Br_2 and obtained the *p*-bromo-substituted compound **13**. Such a bromo-substituted compound **13** showed a better property in crystallization and X-ray diffraction. Slow evaporation of a solution of **13** in $CS_2/CHCl_3/C_2H_4Cl_2$ (1:1:1) at 5 °C gave red crystals suitable for X-ray diffraction analysis.

The X-ray structure of **13** is shown in Figure 3. It is quite similar to the structure of **6a** in Figure 2. The major difference is the elimination of the amide group in **6a** and formation of the new carbonyl group. An important feature of the present structure is the location of the hydroxyl group, which is on the side close to the imino group. There is a hydrogen bond between the imino nitrogen and the OH group. The N···O bond length is 2.867 Å, and the bond angle O−H−N is 131°. On the basis of the location of the OH group shown here, the hydroxyl group in compounds **7a**, **10**, and **12** can also be assigned in the same way because they are the precursors. Just like the conversion of **6** to **7** discussed earlier, compound **11** can be reduced to **12** by CuBr too (Scheme 13).

Scheme 14

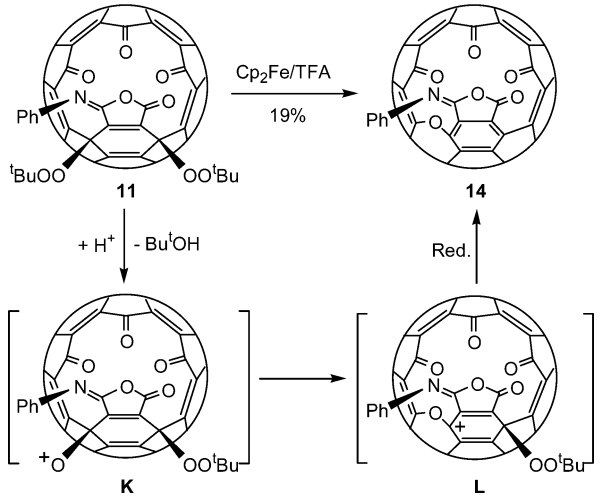

Formation of Water-Encapsulated Complexes. In the ^1H NMR spectra of the 18-membered-ring orifice compounds **11**, **12**, and **13**, minor impurity signals were observed at −13.07, −13.11, and −13.13 ppm, respectively. In light of the water-encapsulated fullerene derivatives reported by Iwamatsu et al.,[11d,f] we assigned the signal to encapsulated water. Chemical shifts of encapsulated H_2O for the present complexes are slightly upfield-shifted compared to that of Iwamatsu's compound (−11.4 ppm).[11d] The encapsulation ratios for compounds **11**, **12**, and **13** were low at less than 5% as estimated from the integral ratio. Heating a solution of **13** in toluene/water at 80 °C for 5 h could increase the water content to 78%,[11d] but a further increase was difficult even by heating the solution at higher temperature.

In an effort to expand the orifice for more efficient water encapsulation, compound **11** was treated with ferrocene in the presence of trifluoroacetic acid (Scheme 14). The reaction removed the two *tert*-butyl peroxy groups and inserted an oxygen atom into the rim of the orifice to give **14** with a 19-membered-ring orifice. The regioselectivity of this reaction suggests that cleavage of the O−O bond of the *tert*-butyl peroxy group closer to the imino group probably initiates the reaction. Formation of **13** with the OH group closer to the imino group from its bis(*tert*-butyl peroxy) precursor **11** also indicates that the *tert*-butyl peroxy group closer to the imino group is more reactive. Rearrangement of the oxonium intermediate **K** then inserts the oxygen atom into the rim of the orifice. Release of steric strain should be the driving force for the rearrangement. Reduction and elimination of the second *tert*-butyl peroxy group in **L** give **14** with an aromatic benzene ring fused with the isomaleimide moiety.

As expected compound **14** with a slightly expanded orifice is a more efficient water trap than compounds **11**, **12**, and **13**. Its ^1H NMR showed an encapsulated water signal at −12.8 ppm.

(20) (a) Leffler, J. E.; Bond, W. B. *J. Am. Chem. Soc.* **1956**, *78*, 335. (b) Kutyrev, A. A.; Ovrutskii, D. G.; Moskva, V. V. *Zh. Obshch. Khim.* **1988**, *58*, 790.

The integral ratio indicates 57% water content for a freshly prepared sample at room temperature. Keeping the NMR sample in the refrigerator for several days at −20 °C could increase the water content to 88%.

The chemical shift of the OH group in empty **13** appears at higher field than that of the water-encapsulated H_2O@**13**. The difference is 6.6 Hz centered at 6.69 ppm for a 1:3 mixture of **13** and H_2O@**13** in $CDCl_3$ on 300 MHz NMR equipment. The same phenomenon has been reported before by Komatsu and Murata et al. for their cage-opened compounds.[10j] Downfield shifts of 0.36 and 1.9 Hz were observed for He- and H_2-encapsulated complexes compared to the corresponding empty compounds.[10j] The difference is a clear indication of the nonbonding interaction between the encapsulated species and the fullerene cage, as pointed out by Komatsu and Murata et al.[10j] The larger chemical difference observed here indicates that the nonbonding interaction in H_2O@**13** is stronger than those in Komatsu's compounds with encapsulated H_2 and He.

Large upfield shifts have been observed upon functionalization of $H_2@C_{60}$[21] and $He@C_{60}$.[22] For example, the ^1H signal of the encapsulated H_2 of $H_2@C_{60}(H)Ph_5$ appears at −10.39 ppm as opposed to −1.44 ppm for $H_2@C_{60}$; the ^3He signal of the encapsulated He of $He@C_{60}(Cl)Ph_5$ appears at −15.14 ppm as opposed to −6.4 ppm for $He@C_{60}$. The phenomenon can be explained as a result of the greater delocalization arising from the decrease in strain.[22] In addition, pentaaddition destroys 6 deshielding [5]radialene moieties out of the total of 12 in [60]-fullerene, but only 5 shielding cyclohexatriene moieties out of the total of 20. Therefore, the overall outcome of these structural changes must result in strong shielding of the center of the cage, as pointed out by Nakamura et al.[21] ^1H NMR chemical shifts of water in H_2O@**13** and H_2O@**14** are comparable to those in the pentaadducts of $H_2@C_{60}$ and $He@C_{60}$, indicating that structural changes in the center pentagon have little effect on the aromaticity[23] of the rest of the cage.

Iwamatsu et al. carried out a series of NMR and ESI-MS experiments with their cage-opened compounds to investigate various factors on the water encapsulation and release property.[11d] Similar phenomena were observed for the present compounds. Addition of D_2O to the $CDCl_3$ solution of H_2O@**13** and H_2O@**14** resulted in disappearance of the characteristic encapsulated water signal. The exchange rate is faster for H_2O@**14** with a slightly larger orifice. The water signal of H_2O@**14** at −12.8 ppm disappeared completely in less than 1 h after addition of D_2O at room temperature, but the intensity of the water signal for H_2O@**13** only decreased from 78% to 60% after 7 h at room temperature.

In the ESI (negative mode) mass spectrum of empty **13**, the molecular ion was observed as the base peak. In the spectrum of H_2O@**13**, the molecular ion peak of H_2O@**13** was observed as the base peak together with empty **13**. The intensity ratio is 100:23 corresponding to 81% water encapsulation, which is close to the ^1H NMR derived value of 78%. On the other hand, only the molecular ion peak of empty **14** was observed in the spectrum of H_2O@**14**. Therefore, the larger orifice of **14** can incorporate water more efficiently and also release water more readily.

X-ray Structures of Water-Encapsulated Complexes. Single crystals of H_2O@**13** and H_2O@**14** were obtained by storing their $CDCl_3$ solution in the NMR tube at −20 °C. Their X-ray structures at 200 K are shown in Figure 1. In both cases, the encapsulated water molecule was observed directly. The water encapsulation ratios were 83% and 96%, respectively, for H_2O@**13** and H_2O@**14** as determined from the refined occupancy in the structure refinement. These values agree well with those from the ^1H NMR spectra (78% for H_2O@**13** and 88% for H_2O@**14**).

The locations of the two hydrogen atoms of the encapsulated water molecule in H_2O@**14** were derived from the differential Fourier map.[24] One hydrogen atom pointing toward the opening appears evident, but the other one is not. Therefore, at 200 K, rotation of the encapsulated water was partially frozen toward its most favored orientation. Rapid rotation of the water molecule was observed at room temperature by ^1H NMR as indicated by a sharp singlet for the encapsulated water protons.

In the case of H_2O@**13** the encapsulated water molecule still rotates very fast even at 200 K. The hydrogen atoms of the encapsulated water could not be located from the X-ray structure determination. This indicates that the rotation barrier of water in H_2O@**13** is lower than that in H_2O@**14**. The phenomenon may be due to the different locations of the encapsulated water. The distance of the water oxygen atom from the center of the bottom pentagon is 3.30 Å for H_2O@**13** and 3.67 Å for H_2O@**14**, so the water molecule in H_2O@**14** is closer to the orifice, thus having a higher steric hindrance of rotation. In agreement with this feature, the ellipsoid shape of the water oxygen in H_2O@**14** shows vibration along the direction toward the orifice, but the same vibration in H_2O@**13** is very weak (Figure 4).

What is the driving force for water encapsulation? The process appeared to be thermodynamically favorable since even storing the solution of **14** at −20 °C can increase the water content. A possible explanation is that the empty cavity of the fullerene cage is electron deficient. Due to the curvature of the fullerene cage, the electron density is greater on the outer surface than on the more crowded inner surface to minimize electron repulsion.[1a] The presence of the multiple carbonyl groups in the present cage-opened compounds increases the electron deficiency through their electron-withdrawing effect. Therefore, the cavity acts like an empty orbital of a Lewis acid. This "Lewis acid and Lewis base" interaction between the encapsulated water and the cavity would cause a downfield shift for the water ^1H NMR signal, but this effect is relatively small compared to the strong shielding effect of the cage structure (see the earlier discussion); thus, upfield-shifted ^1H NMR signals for H_2O@**13** and H_2O@**14** were observed. Under the ESI conditions (negative mode) reduction of the cage diminishes its "Lewis acidity"; thus, the encapsulated water is forced out from H_2O@**14**, which has a larger orifice and lower barrier for water release compared to

(21) Matsuo, Y.; Isobe, H.; Tanaka, T.; Murata, Y.; Murata, M.; Komatsu, K.; Nakamura, E. *J. Am. Chem. Soc.* **2005**, *127*, 17148.
(22) Birkett, P. R.; Bühl, M.; Khong, A.; Saunders, M.; Taylor, R. *J. Chem. Soc., Perkin Trans. 2* **1999**, 2037.
(23) Bühl, M.; Hirsch, A. *Chem. Rev.* **2001**, *101*, 1153.
(24) For X-ray structure of H_2-encapsulated compounds see ref 21 and Sawa, H.; Wakabayashi, Y.; Murata, Y.; Murata, M.; Komatsu, K. *Angew. Chem., Int. Ed.* **2005**, *44*, 1981.

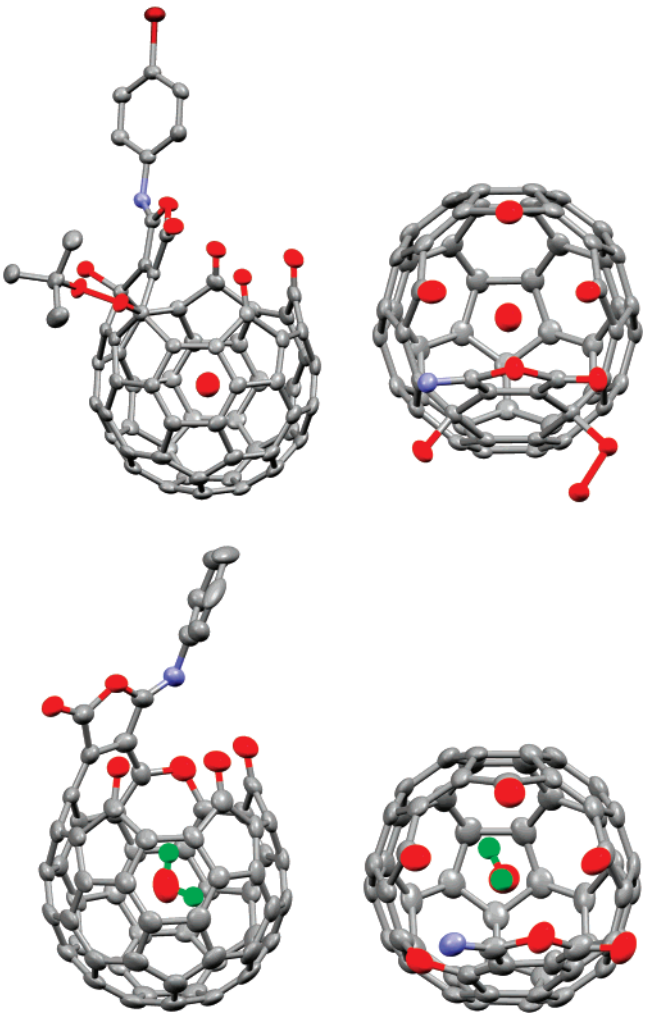

Figure 4. X-ray structures of compounds H_2O@**13** (above) and H_2O@**14** (below). Ellipsoids were drawn at the 50% level. For clarity carbon-bonded hydrogen atoms and aryl and ^{t}Bu groups in the top views (right) are not shown. The water hydrogen atoms of H_2O@**13** could not be defined. Key: gray, carbon; red, oxygen; blue, nitrogen; green, hydrogen; dark red, bromine.

13. Water-encapsulated pristine C_{60} complex $H_2O@C_{60}$ has been predicted to be stable by theoretical calculations.[25]

Summary

A total of five fullerene carbon−carbon bonds were cleaved and one skeleton carbon atom was eliminated from C_{60} through an eight-step reaction sequence as outlined in Scheme 15. The first cage-opening process involves a dioxetane intermediate formed by photoinduced homolysis of the ^{t}Bu−O bond. Oxidation of the vicinal fullerene hydroxyl moiety by DIB is a key step in the second stage. Strain release is the driving force for the domino rearrangement step in which the fourth fullerene carbon−carbon bond is cleaved. Mild decarboxylation in the final step indicates that the *tert*-butyl peroxy groups are versatile precursors for fullerene skeleton modification. The yield of the second photolysis step is relatively low (25%) compared to that of most other steps in the sequence (around 60%). The total yield of the final product C_{59} triketone **12** is 1.12%. All the

Scheme 15

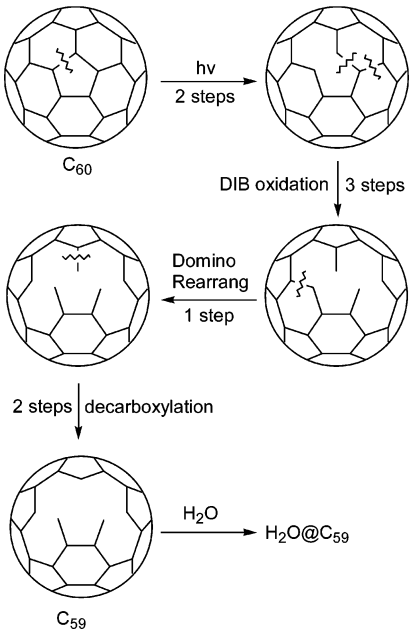

reactions were carried out under mild reaction conditions (temperature below 40 °C and in air) and employing flash chromatography purification procedures. The present results provide a new method for multiple fullerene carbon−carbon bond cleavage.

The open-cage [59]fullerenones are found to be excellent hosts for water. The X-ray structures of compounds H_2O@**13** and H_2O@**14** provide conclusive evidence for water encapsulation in open-cage C_{60} derivatives, supporting the previous spectroscopic data derived result by Iwamatsu et al.[11d] Further work is in progress to prepare truncated fullerene derivatives (norfullerenes) starting from compounds prepared here and to incorporate other atoms or molecules into the cavity of open-cage fullerene derivatives.

Experimental Section

All the reagents were used as received. Benzene used for the reactions was distilled on potassium under nitrogen. Dichloromethane was distilled on phosphorus pentoxide. Other solvents were used as received. The reactions were carried out in air. Compound **1** was prepared according to the improved procedure in ref 17. The NMR spectra were obtained at 25 °C unless noted. Compounds not shown below are included in the Supporting Information.

Caution: A large amount of peroxides is involved in some of the reactions. Care must be taken to avoid possible explosion.

Open-Cage Fullerene Derivative 2. A solution of compound **1** (2.9 g, 1.9 mmol) and I_2 (500 mg, 2.0 mmol) in benzene (500 mL) was irradiated by three LED blue-color lamps (470 nm, two 15 W and one 5 W) for 1.5 h. The resulting solution was treated by $Na_2S_2O_3$ to reduce excess iodine (1.0 g, 6.3 mmol dissolved in 10 mL of H_2O). The organic layer was evaporated, and the residual was dissolved in toluene (5 mL). The toluene solution was chromatographed on a silica gel column (50 × 150 mm) eluting with toluene. The first band was a mixture of several uncharacterized products. The second red band was collected and evaporated to give compound **2** (650 mg, 0.6 mmol, 25%). For spectroscopic data, see ref 18.

Open-Cage Fullerene Derivative 3a. To a stirred solution of compound **2** (650 mg, 0.58 mmol) in CH_2Cl_2 (300 mL) was added $B(C_6F_5)_3$ (78 mg, 0.15 mmol) at 30 °C. After 5 min, the solution was directly chromatographed on a silica gel column (70 × 50 mm) eluting

(25) (a) Williams, C. I.; Whitehead, M. A.; Pang, L. *J. Phys. Chem.* **1993**, *97*, 11652. (b) Shameema, O.; Ramachandran, C. N.; Sathyamurthy, N. *J. Phys. Chem. A* **2006**, *110*, 2.

with toluene/petroleum ether/AcOEt (10:10:1). The first band was collected as the unreacted **2** (50 mg, 0.044 mmol, 8%). Then the elution was changed to toluene/petroleum ether/AcOEt (5:5:1). A red band was collected and evaporated to give **3a** (399 mg, 0.35 mol, 60%). ^{1}H NMR (400 MHz, $CDCl_3$): δ 6.28 (s, 1H), 4.88 (s, 1H), 1.38 (s, 9H), 1.37 (s, 9H), 1.32 (s, 9H), 1.27 (s, 9H). ^{13}C NMR (100 MHz, $CDCl_3$): all signals represent 1C except as noted; δ 198.97, 194.04, 149.18, 149.13, 149.02, 148.94, 148.88, 148.86, 148.79 (2C), 148.69, 148.67, 148.52 (2C), 148.43, 148.38, 148.26 (2C), 148.20, 148.17 (2C), 148.01, 147.89, 147.66, 147.40, 147.34, 146.69, 146.39, 145.09, 144.74, 144.72, 144.53, 144.22, 144.14, 143.96, 143.91, 143.87, 143.29 (2C), 142.67, 142.60, 142.50, 142.37, 141.29, 140.99, 140.77, 140.41, 140.33, 140.31, 140.22, 140.16, 138.08, 135.47, 134.85, 90.57 (1C, sp^3), 89.33 (1C, sp^3), 86.57 (1C, sp^3), 82.78 (1C, sp^3), 82.35 (1*C*$(CH_3)_3$), 82.21 (1C, sp^3), 81.95 (1*C*$(CH_3)_3$) 81.86 (1*C*$(CH_3)_3$), 81.73 (1*C*$(CH_3)_3$), 80.68 (1C, sp^3), 26.67 ($3CH_3$), 26.54 ($6CH_3$), 26.37 ($3CH_3$). FT-IR (microscope): 3461, 3342, 2979, 2930, 1732, 1388, 1364, 1193, 1057, 1004, 871, 733 cm^{-1}. ESI-MS (Bruker Esquire): *m*/*z* (rel intens) 1160 (100, M + NH_4^+).

Open-Cage Fullerene Derivative 3b. To a stirred solution of compound **2** (29 mg, 0.026 mmol) in benzene (5 mL) was added anhydrous $FeCl_3$ (5 mg, 0.031 mmol) at room temperature. After 5−10 min, the solution was directly chromatographed on a silica gel column (20 × 50 mm) eluting with toluene/petroleum ether/AcOEt (10:10:1). The first band was collected as the unreacted **2** (trace). The second red band was collected and evaporated to give **3b** (25 mg, 0.022 mmol, 84%). ^{1}H NMR (400 MHz, $CDCl_3$): δ 5.93 (s, 1H), 1.39 (s, 18H), 1.32 (s, 9H), 1.29 (s, 9H). ^{13}C NMR (100 MHz, $CDCl_3$): all signals represent 1C except as noted; δ 196.89, 193.70, 149.38, 149.18, 149.08, 149.01, 148.99 (2C), 148.93, 148.80 (2C), 148.78, 148.60, 148.50 (2C), 148.48, 148.46, 148.44, 148.34, 148.24, 148.22, 148.03, 147.88, 147.48, 147.39, 146.73, 146.47, 145.65, 145.29, 144.89, 144.79, 144.60, 144.39, 144.08, 144.04, 143.98, 143.89, 143.37, 143.12 (2C), 142.82, 142.50, 141.39, 141.25, 141.13, 140.55, 140.34 (2C), 140.22, 139.71, 139.15, 138.66, 135.48, 134.59, 90.70 (1C, sp^3), 89.13 (1C, sp^3), 86.50 (1C, sp^3), 82.51 (1*C*$(CH_3)_3$), 82.24 (1C, sp^3), 82.12 (1*C*$(CH_3)_3$), 82.03 (2*C*$(CH_3)_3$), 80.86 (1C, sp^3), 76.16 (1C, sp^3), 26.75 ($3CH_3$), 26.64 ($3CH_3$), 26.61 ($3CH_3$), 26.41 ($3CH_3$). FT-IR (microscope): 3408, 2979, 2929, 1731, 1388, 1364, 1192, 1006, 908, 733 cm^{-1}. ESI-MS (Bruker Esquire): *m*/*z* (rel intens) 1178 (100, M + NH_4^+).

Closed-Cage Fullerene Derivative 4a. Compound **3a** (399 mg, 0.35 mmol) was dissolved in CH_2Cl_2 (10 mL), and aniline (326 mg, 3.5 mmol) was added. The solution was stirred at 30 °C. After 3 h, the CH_2Cl_2 was evaporated and the residual was dissolved in 5 mL of mixed solvent toluene/petroleum ether/AcOEt (5:5:1). Then the solution was chromatographed on a silica gel column (35 × 200 mm) eluting with the same solvent. The first band was collected as the unreacted **3a** (10 mg, 0.0088 mmol, 3%). The red band was collected and evaporated to give **4a** (366 mg, 0.30 mmol, 85%). ^{1}H NMR (400 MHz, $CDCl_3$): δ 7.52−7.45 (2H), 7.32−7.26 (2H), 6.90−6.87 (1H), 6.88 (s, 1H), 6.42 (s, 1H), 5.65 (s, 1H), 4.95 (s, 1H), 1.40 (s, 9H), 1.36 (s, 9H), 1.26 (s, 9H), 0.98 (s, 9H). ^{13}C NMR (100 MHz, $CDCl_3$): all signals represent 1C except as noted; δ 149.12 (2C), 148.96, 148.92, 148.87, 148.80, 148.76, 148.71, 148.69, 148.63, 148.58 (2C), 148.52, 148.48, 148.34, 148.29, 148.14, 147.93, 147.72, 147.69, 147.63, 147.58, 147.12, 146.31, 145.74, 145.57, 144.98, 144.83, 144.61, 144.58, 144.52, 144.48, 144.10, 144.04, 144.01, 143.73, 143.72, 143.53, 143.32, 143.25, 143.18, 142.21, 141.37, 141.20, 140.79, 140.49, 138.22, 138.18, 137.92, 137.26, 136.35, 134.41, 129.23, 128.47 (2CH-aryl), 119.04 (CH-aryl), 117.51 (2CH-aryl), 98.61 (1C, sp^3), 93.65 (1C, sp^3), 91.31 (1C, sp^3), 88.08 (1C, sp^3), 84.35 (1C, sp^3), 83.00 (1*C*$(CH_3)_3$), 82.40 (1*C*$(CH_3)_3$), 81.93 (1C, sp^3), 81.74 (1*C*$(CH_3)_3$), 81.41 (1*C*$(CH_3)_3$), 77.90 (1C, sp^3), 72.03 (1C, sp^3), 26.79 ($6CH_3$), 26.67 ($3CH_3$), 26.21 ($3CH_3$). FT-IR (microscope): 3489, 3419, 2977, 2930, 1602, 1501, 1387, 1364, 1189, 1055, 1006, 757 cm^{-1}. ESI-MS (Bruker Esquire): *m*/*z* (rel intens) 1236 (100, M + H^+).

Closed-Cage Fullerene Derivative 4b. Compound **3a** (121 mg, 0.11 mmol) was dissolved in CH_2Cl_2 (5 mL), and anisidine (65 mg, 0.53 mmol) was added. The solution was stirred at 30 °C. After 1 h, the solution was directly chromatographed on a silica gel column (20 × 150 mm) eluting with toluene/petroleum ether/AcOEt (5:5:1). The first band was collected as the unreacted **3a** (trace). The red band was collected and evaporated to give **4b** (114 mg, 0.090 mmol, 85%). ^{1}H NMR (400 MHz, $CDCl_3$): δ 7.43−7.41 (2H), 6.93−6.90 (2H), 6.61 (s, 1H), 6.39 (s, 1H), 5.55 (s, 1H), 4.93 (s, 1H), 3.83 (s, 3H), 1.41 (s, 9H), 1.36 (s, 9H), 1.25 (s, 9H), 1.02 (s, 9H). ^{13}C NMR (100 MHz, $CDCl_3$): all signals represent 1C except as noted; δ 153.30, 149.15 (2C), 148.99, 148.95, 148.88, 148.84, 148.79, 148.74, 148.71, 148.65 (2C), 148.61, 148.53, 148.50, 148.36, 148.33, 148.15, 147.96, 147.75, 147.74, 147.68, 147.67, 147.13, 146.37, 145.84, 145.60, 144.97, 144.86, 144.63 (2C), 144.54, 144.49, 144.13, 144.08, 143.97, 143.74 (2C), 143.60, 143.35, 143.28, 143.21, 142.29, 141.43, 141.26, 140.80, 140.49, 138.49, 138.27, 137.89, 137.84, 137.29, 136.50, 134.44, 118.93 (2CH-aryl), 114.24 (2CH-aryl), 98.60 (1C, sp^3), 93.58 (1C, sp^3), 91.38 (1C, sp^3), 88.48 (1C, sp^3), 84.38 (1C, sp^3), 83.00 (1*C*$(CH_3)_3$), 82.31 (1*C*$(CH_3)_3$), 81.95 (1C, sp^3), 81.76 (1*C*$(CH_3)_3$), 81.45 (1*C*$(CH_3)_3$), 77.94 (1C, sp^3), 72.04 (1C, sp^3), 55.95 (1(OCH_3)), 26.79 ($6CH_3$), 26.70 ($3CH_3$), 26.35 ($3CH_3$). FT-IR (microscope): 3484, 3413, 2977, 2930, 2869, 1742, 1513, 1388, 1365, 1242, 1189, 1049, 1001, 756 cm^{-1}. ESI-MS (Bruker Esquire): *m*/*z* (rel intens) 1266 (100, M + H^+).

Closed-Cage Fullerene Derivatives 4l and 4l′. To a solution of compound **3e** (90 mg, 0.080 mmol) in CH_2Cl_2 (5 mL) was added NH_3-(g) at room temperature for 5 min. The solution was evaporated, and the residual was dissolved in and eluted with toluene/AcOEt (10:3) on a silica gel column (35 × 50 mm). The first band was collected and evaporated to give **4l** (25 mg, 0.022 mmol, 27%). The second band was collected and evaporated to give **4l′** (61 mg, 0.053 mmol, 67%).

Data for 4l. ^{1}H NMR (400 MHz, $CDCl_3$): δ 6.36 (s, 1H), 5.24 (s, 1H), 3.83 (s, 2H), 1.42 (s, 9H), 1.35 (s, 18H), 1.28 (s, 9H). ^{13}C NMR (100 MHz, $CDCl_3$): all signals represent 1C except as noted; δ 149.35, 149.09, 149.05, 149.01 (2C), 148.77, 148.73, 148.65 (2C), 148.57, 148.44, 148.33 (3C), 148.29 (2C), 148.21, 148.19, 147.96, 147.74, 147.66, 147.64, 147.59, 147.56, 146.12, 145.54 (2C), 145.34, 145.22, 144.86, 144.77, 144.69 (2C), 144.55, 144.40, 144.14, 143.67, 143.62, 143.49, 143.45, 143.14, 143.05, 141.48, 141.44, 141.04, 140.90, 140.21, 138.65, 136.80, 136.38, 134.27, 131.35, 96.46 (1C, sp^3), 92.84 (1C, sp^3), 92.68 (1C, sp^3), 91.49 (1C, sp^3), 83.90 (1C, sp^3), 83.10 (1*C*$(CH_3)_3$), 82.41 (1*C*$(CH_3)_3$), 82.15 (1C, sp^3), 81.45 (1*C*$(CH_3)_3$), 81.36 (1*C*$(CH_3)_3$), 73.70 (1C, sp^3), 54.33 (CH), 27.00 ($3CH_3$), 26.73 ($3CH_3$), 26.69 ($3CH_3$), 26.62 ($3CH_3$). FT-IR (microscope): 3511, 3458, 2977, 2928, 1473, 1458, 1387, 1364, 1191, 1070, 1041, 1021, 990, 868, 756 cm^{-1}. ESI-MS (Bruker Esquire): *m*/*z* (rel intens) 1144 (100, M + H^+).

Data for 4l′. ^{1}H NMR (400 MHz, $CDCl_3$): δ 7.60 (s, 1H), 5.08 (s, 1H), 3.81 (s, 2H), 1.41 (s, 9H), 1.37 (s, 9H), 1.30 (s, 18H). ^{13}C NMR (100 MHz, $CDCl_3$): all signals represent 1C except as noted; δ 149.17, 149.01, 148.94 (3C), 148.88, 148.78, 148.72, 148.59 (2C), 148.47, 148.41 (2C), 148.35, 148.26 (3C), 147.97, 147.69, 147.64, 147.40, 147.27, 146.67, 145.86, 145.63, 145.17, 145.09, 144.95, 144.79, 144.70, 144.37, 144.27, 144.08, 143.95, 143.90, 143.84, 143.68, 143.42, 142.55, 141.98, 141.77, 141.13, 140.71, 140.14, 138.78, 138.47, 137.81, 99.38 (1C, sp^3), 92.96 (1C, sp^3), 91.02 (1C, sp^3), 88.24 (1C, sp^3), 83.99 (1C, sp^3), 82.49 (1*C*$(CH_3)_3$), 82.10 (1*C*$(CH_3)_3$), 82.04 (1*C*$(CH_3)_3$), 81.71 (1*C*$(CH_3)_3$), 81.35 (1C, sp^3), 73.26 (1C, sp^3), 53.57 (CH), 26.88 ($3CH_3$), 26.81 ($6CH_3$), 26.73 ($3CH_3$).

Spectra at 323 K. ^{1}H NMR (400 MHz, $CDCl_3$): δ 6.84 (s, 1H), 6.61 (s, 1H), 5.11 (s, 1H), 3.43 (s, 2H), 1.40(s, 9H), 1.38 (s, 9H), 1.30 (s, 18H). ^{13}C NMR (100 MHz, $CDCl_3$): all signals represent 1C except as noted; δ 149.14, 148.97 (3C), 148.94, 148.89, 148.85, 148.75 (2C), 148.71, 148.60, 148.55, 148.41 (3C), 148.32, 148.31, 148.29 (3C), 148.23, 148.00, 147.68, 147.64, 147.46, 147.45, 146.17, 145.80, 145.56, 145.23, 145.11, 144.89, 144.76, 144.68, 144.64, 144.35, 144.02 (2C), 143.83, 143.74, 143.61, 143.41, 142.77, 141.68, 141.40, 141.29, 140.73,

140.10, 139.21, 139.10, 137.78, 136.27, 99.35 (1C, sp^3), 92.89 (1C, sp^3), 91.34 (1C, sp^3), 88.43 (1C, sp^3), 84.09 (1C, sp^3), 82.15 (1*C*(CH_3)$_3$), 81.91 (2*C*(CH_3)$_3$), 81.78 (1*C*(CH_3)$_3$), 81.60 (1C, sp^3), 73.20 (1C, sp^3), 53.91 (CH), 26.83 ($3CH_3$), 26.80 ($3CH_3$), 26.75 ($3CH_3$), 26.69 ($3CH_3$). FT-IR (microscope): 3500, 3388, 2978, 2927, 1473, 1457, 1387, 1364, 1191, 1040, 1021, 868, 757 cm^{-1}. ESI-MS (Bruker Esquire): *m*/*z* (rel intens) 1144 (100, M + H^+).

Crystals suitable for X-ray diffraction were obtained from slow evaporation of **4l′** in a mixture of CS_2, toluene, and ethanol (1:1:1). Crystal system, space group: monoclinic, *P*2(1)/*c*. Unit cell dimensions: a = 24.831(5) Å, α = 90°, b = 13.989(3) Å, β = 111.70(3)°, c = 19.483(4) Å, γ = 90°, volume 6288(2) $Å^3$. Final *R* indices [$I > 2\sigma(I)$]: R1 = 0.0796, wR2 = 0.1678.

Open-Cage Fullerene Derivative 5a. To the solution of compound **4a** (366 mg, 0.30 mmol) in benzene (150 mL)/CH_3OH (1.5 mL) was added DIB (334 mg, 1.0 mmol) at 35 °C. After being stirred for 30 min, the solution was directly chromatographed on a silica gel column (50 × 100 mm) eluting with toluene/petroleum ether/AcOEt (10:10:1). The first red band was collected and evaporated to give **5a** (220 mg, 0.18 mmol, 60%). ^{1}H NMR (400 MHz, $CDCl_3$): δ 7.75−7.73 (2H), 7.48−7.44 (2H), 7.29−7.26 (1H), 1.38 (s, 9H), 1.34 (s, 9H), 1.22 (s, 9H), 1.18 (s, 9H). ^{13}C NMR (100 MHz, $CDCl_3$): all signals represent 1C except as noted; δ 191.25, 156.38, 154.23, 152.61, 150.48, 150.33, 150.28, 150.15, 149.89, 149.54, 149.25, 149.07, 149.04, 148.94, 148.86, 148.55, 148.34, 148.25, 148.14, 148.05, 147.90, 147.81, 147.62, 147.21, 147.16, 146.96, 146.59, 145.53, 145.42, 144.92, 144.83, 144.76, 144.68, 144.16, 144.02, 143.85, 143.52, 143.42, 143.20, 142.87, 142.08, 141.96, 141.87, 141.40, 141.04, 140.85, 140.65, 139.80, 139.43, 139.34, 139.01, 138.54, 137.70, 137.10, 133.46, 131.47, 130.92, 128.51 (2CH-aryl), 126.17 (CH-aryl), 122.42 (2CH-aryl), 95.02 (1C, sp^3), 91.18 (1C, sp^3), 88.52 (1C, sp^3), 82.65 (1*C*(CH_3)$_3$), 82.27 (1*C*(CH_3)$_3$), 82.07 (1*C*(CH_3)$_3$), 81.49 (1*C*(CH_3)$_3$), 80.63 (1C, sp^3), 26.87 ($3CH_3$), 26.76 ($3CH_3$), 26.72 ($3CH_3$), 26.42 ($3CH_3$). FT-IR (microscope): 2979, 2930, 1860, 1799, 1746, 1364, 1192, 1106, 1066, 1024, 734 cm^{-1}. ESI-MS (Bruker Esquire): *m*/*z* (rel intens) 1232 (100, M + H^+).

Open-Cage Fullerene Derivative 5b. To the solution of compound **4b** (43 mg, 0.034 mmol) in benzene (15 mL)/CH_3OH (0.15 mL) was added DIB (38 mg, 0.12 mmol) at 35 °C. After being stirred for 30 min, the solution was directly chromatographed on a silica gel column (50 × 100 mm) eluting with toluene/petroleum ether/AcOEt (10:10:1). The first red band was collected and evaporated to give **5b** (22 mg, 0.017 mmol, 50%). ^{1}H NMR (400 MHz, $CDCl_3$): δ 7.77−7.75 (2H), 7.02−7.00 (2H), 3.92 (s, 3H), 1.36 (s, 9H), 1.33 (s, 9H), 1.27 (s, 9H), 1.19 (s, 9H). ^{13}C NMR (100 MHz, $CDCl_3$): all signals represent 1C except as noted; δ 191.15, 158.66, 156.22, 152.46, 152.04, 150.42, 150.26, 150.21, 150.07, 149.82, 149.46, 149.17, 149.00, 148.95, 148.86, 148.78, 148.47, 148.28, 148.19, 148.07, 147.98, 147.81, 147.74, 147.53, 147.15, 147.10, 146.54, 145.37, 145.34, 144.86, 144.81 (2C), 144.64, 144.15, 143.97, 143.79, 143.48, 143.37, 143.10, 142.88, 141.98, 141.95, 141.66, 141.49, 140.93, 140.77, 140.57, 140.50, 139.74, 139.35, 139.32, 139.12, 138.93, 138.55, 137.66, 137.18, 132.93, 131.38, 124.46 (2CH-aryl), 113.93 (2CH-aryl), 94.83 (1C, sp^3), 91.21 (1C, sp^3), 88.51 (1C, sp^3), 82.54 (1*C*(CH_3)$_3$), 82.15 (1*C*(CH_3)$_3$), 82.01 (1*C*(CH_3)$_3$), 81.36 (1*C*(CH_3)$_3$), 80.70 (1C, sp^3), 55.43 (1(O*C*H_3)), 26.80 ($3CH_3$), 26.73 ($3CH_3$), 26.64 ($3CH_3$), 26.43 ($3CH_3$). FT-IR (microscope): 2980, 2931, 1859, 1798, 1745, 1504, 1364, 1248, 1192, 1106, 1066, 1025, 733 cm^{-1}. ESI-MS (Bruker Esquire): *m*/*z* (rel intens) 1284 (100, M + Na^+).

Open-Cage Fullerene Derivatives 6a and 7a. To the solution of compound **5b** (40 mg, 0.032 mmol) in CH_2Cl_2 (10 mL) was added anisidine (20 mg, 0.16 mmol). After being stirred at room temperature for 24 h, the solution was directly chromatographed on a silica gel column (20 × 50 mm) eluting with toluene/petroleum ether/AcOEt (10:10:1). The first band was collected and evaporated to give the unreacted **5b** (3 mg, 0.0024 mmol, 8%). The second band was collected and evaporated to give a mixture of **6a** and **7a** (24 mg). Then this mixture was further eluted with toluene/AcOEt (30:1) on a silica gel column (20 × 100 mm). The first band was collected and evaporated to give **7a** (6 mg, 0.0048 mmol, 15%). The second band was collected and evaporated to give **6a** (14 mg, 0.011 mmol, 34%).

Data for 6a. ^{1}H NMR (400 MHz, $CDCl_3$): δ 8.93 (s, 1H), 7.68−7.65 (2H), 7.09−7.07 (2H), 7.03−7.01 (2H), 6.85−6.83 (2H), 3.94 (s, 3H), 3.89 (s, 3H), 1.27 (s, 9H), 1.23 (s, 9H), 1.18 (s, 9H). ^{13}C NMR (100 MHz, $CDCl_3$): all signals represent 1C except as noted; δ 185.56, 184.20, 162.52, 160.97, 157.86, 157.80, 150.72, 150.65, 150.07, 150.00, 149.59, 149.34, 149.32 (2C), 149.01 (2C), 149.73, 148.62, 148.60, 148.39, 148.26, 148.12, 148.05, 147.75, 147.64, 147.56 (2C), 146.42, 146.38, 145.83, 145.78, 145.68, 145.16, 144.95, 144.83, 144.72, 144.59, 144.13, 142.62, 142.43, 142.39, 142.16, 141.28 (2C), 141.16, 140.90, 140.87, 140.67, 140.55, 140.14, 139.96, 139.71, 138.20, 136.53, 135.87, 135.67, 134.52, 133.90, 133.77, 133.61, 128.73, 126.64 (2CH-aryl), 125.99 (2CH-aryl), 114.43 (2CH-aryl), 113.78 (2CH-aryl), 92.23 (1C, sp^3), 84.76 (1C, sp^3), 84.38 (1C, sp^3), 83.10 (1*C*(CH_3)$_3$), 81.53 (1*C*(CH_3)$_3$), 81.19 (1*C*(CH_3)$_3$), 55.48 (1(O*C*H_3)), 55.35 (1(O*C*H_3)), 26.89 ($3CH_3$), 26.81 ($3CH_3$), 26.80 ($3CH_3$). FT-IR (microscope): 3415, 2979, 2929, 1802, 1748, 1699, 1537, 1511, 1505, 1364, 1246, 1189, 756 cm^{-1}. ESI-MS (Bruker Esquire): *m*/*z* (rel intens) 1311 (100, M + H^+).

Crystals suitable for X-ray diffraction were obtained from slow evaporation of **6a** in a mixture of CS_2, $CHCl_3$, and CH_3OH (1:3:1). Crystal system, space group: triclinic, $P\bar{1}$. Unit cell dimensions: a = 13.586(3) Å, α = 87.21(3)°, b = 17.026(3) Å, β = 77.50(3)°, c = 17.336(4) Å, γ = 75.58(3)°, volume 3791.8(13) $Å^3$. Final *R* indices [$I > 2\sigma(I)$]: R1 = 0.0789, wR2 = 0.2143.

Data for 7a. ^{1}H NMR (400 MHz, $CDCl_3$): δ 8.98 (s, 1H), 7.71−7.69 (2H), 7.17−7.15 (2H), 7.04−7.02 (2H), 6.89−6.87 (2H), 6.76 (s, 1H), 4.02 (s, 3H), 3.90 (s, 3H), 1.27 (s, 9H), 1.22 (s, 9H). ^{13}C NMR (100 MHz, $CDCl_3$): all signals represent 1C except as noted; δ 185.73, 185.08, 161.65, 161.09, 158.86, 158.03, 150.62, 150.43, 150.12, 150.03, 149.71, 149.52, 149.47, 149.40, 149.20, 149.07, 148.94, 148.82, 148.67, 148.32 (2C), 148.21, 147.98, 147.93, 147.89, 147.62, 147.54, 147.38, 146.36 (2C), 146.31, 145.35, 144.99 (2C), 144.57, 144.30, 143.92, 143.45, 143.00, 142.65, 142.55, 142.27, 142.24, 141.63, 141.42, 141.23, 141.07, 141.03, 140.98, 140.78, 140.10, 139.87, 139.40, 135.95, 134.56 (2C), 134.53, 133.58, 132.91, 131.04, 128.86, 127.77 (2CH-aryl), 126.18 (2CH-aryl), 114.63 (2CH-aryl), 114.10 (2CH-aryl), 92.31 (1C, sp^3), 84.84 (1C, sp^3), 83.17 (1*C*(CH_3)$_3$), 81.79 (1*C*(CH_3)$_3$), 76.34 (1C, sp^3), 55.66 (1(O*C*H_3)), 55.44 (1(O*C*H_3)), 26.78 ($3CH_3$), 26.57 ($3CH_3$). FT-IR (microscope): 3413, 2979, 2931, 2835, 1812, 1747, 1700, 1537, 1510, 1248, 1186, 1040, 734 cm^{-1}. ESI-MS (Bruker Esquire): *m*/*z* (rel intens) 1239 (100, M + H^+).

Open-Cage Fullerene Derivatives 6e and 7e. To the solution of compound **5a** (130 mg, 0.11 mmol) in CH_2Cl_2 (65 mL) was added N_2H_4•H_2O (85%) (7 mg, 0.12 mmol) at 0 °C. The material was rapidly converted to a polar intermediate. Then acetone (638 mg, 11 mmol) was added to the solution. After being stirred for 3 h (the temperature was slowly raised to 15 °C), the solution was directly chromatographed on a silica gel column (20 × 50 mm) eluting with toluene/petroleum ether/AcOEt (5:5:1). The first red band was collected and evaporated to give a mixture of **6e** and **7e** (85 mg). Then this mixture was further eluted with $CHCl_3$/AcOEt (80:1) on a silica gel column (20 × 150 mm). The first band was collected and evaporated to give **7e** (35 mg, 0.032 mmol, 30%). The second band was collected and evaporated to give **6e** (38 mg, 0.032 mmol, 30%).

Data for 6e. ^{1}H NMR (400 MHz, $CDCl_3$): δ 8.42 (s, 1H), 7.72−7.70 (2H), 7.57−7.51 (2H), 7.33−7.29 (1H), 3.92 (s, 2H), 1.27 (s, 9H), 1.24 (s, 18H). ^{13}C NMR (100 MHz, $CDCl_3$): all signals represent 1C except as noted; δ 186.31, 185.96, 164.55, 162.22, 150.76, 150.70, 149.93, 149.92, 149.59, 149.37, 149.33, 149.27, 149.13, 149.08 (2C), 148.67, 148.62, 148.47, 148.41, 148.06 (2C), 147.73, 147.66, 147.57, 147.52, 146.25, 145.97, 145.89, 145.78, 145.75, 145.67, 145.32, 145.15, 145.12, 144.79, 144.48, 144.11, 142.65, 142.53, 142.51, 142.28, 141.44, 141.32, 141.25 (2C), 140.81, 140.79, 140.54, 140.04, 139.99 (2C),

137.23, 136.12, 135.59, 135.47, 135.09, 133.73, 133.45, 129.02 (2CH-aryl), 126.10 (CH-aryl), 123.47 (2CH-aryl), 91.39 (1C, sp^3), 84.73 (1C, sp^3), 84.53 (1C, sp^3), 83.15 (1*C*$(CH_3)_3$), 81.76 (1*C*$(CH_3)_3$), 81.53 (1*C*$(CH_3)_3$), 26.92 ($3CH_3$), 26.82 ($3CH_3$), 26.70 ($3CH_3$). FT-IR (microscope): 3448, 3349, 2980, 2929, 1811, 1747, 1691, 1364, 1189, 1076, 906, 758 cm^{-1}. ESI-MS (Bruker Esquire): *m*/*z* (rel intens) 1190 (100, M + H^+).

Data for 7e. ^1H NMR (400 MHz, $CDCl_3$): δ 8.43 (s, 1H), 7.81−7.79 (2H), 7.59−7.55 (2H), 7.42−7.38 (1H), 6.33 (s, 1H), 4.07 (s, 2H), 1.26 (s, 9H), 1.23 (s, 9H). ^{13}C NMR (100 MHz, $CDCl_3$): all signals represent 1C except as noted; δ 186.71, 186.43, 164.55, 161.62, 150.67, 150.50, 150.20, 149.99, 149.97, 149.54, 149.43 (2C), 149.23, 149.13, 149.05, 148.83, 148.80, 148.68, 148.42, 148.32, 148.29, 147.98, 147.88, 147.62, 147.55, 147.35, 146.29, 145.93, 145.85, 145.47, 145.08, 144.98, 144.52, 144.27, 143.80, 143.30, 142.84, 142.75, 142.60, 142.58, 142.46, 142.10, 141.53, 141.37 (2C), 141.30, 141.24, 141.06, 140.28, 140.15, 140.13, 139.77, 135.06, 134.99, 134.49, 134.27, 134.05, 131.23, 129.33 (2CH-aryl), 127.73 (CH-aryl), 125.44 (2CH-aryl), 91.45 (1C, sp^3), 84.74 (1C, sp^3), 83.19 (1*C*$(CH_3)_3$), 82.02 (1*C*$(CH_3)_3$), 76.57 (1C, sp^3), 26.68 ($3CH_3$), 26.60($3CH_3$). FT-IR (microscope): 3445, 2979, 2928, 1821, 1745, 1691, 1365, 1189, 1077, 908, 734 cm^{-1}. ESI-MS (Bruker Esquire): *m*/*z* (rel intens) 1118 (100, M + H^+).

Open-Cage Fullerene Derivate 8. To the solution of compound **6e** (18 mg, 0.015 mmol) in CH_2Cl_2 (5 mL) was added a $NaNO_2$/hydrochloric acid solution (20 μL, 50 mg of $NaNO_2$ dissolved in 1 mL of hydrochloric acid (1 mol/L)) at 0 °C. After being stirred for 20 min, the solution was directly chromatographed on a silica gel column (20 × 50 mm) eluting with toluene/petroleum ether/AcOEt (10:10:1). The red band was collected and evaporated to give **8** (15 mg, 0.013 mmol, 82%). ^1H NMR (400 MHz, $CDCl_3$): δ 7.74−7.72 (2H), 7.53−7.49 (2H), 7.32−7.28 (1H), 1.26(s, 9H), 1.25 (s, 9H), 1.23 (s, 9H). ^{13}C NMR (100 MHz, $CDCl_3$): all signals represent 1C except as noted; δ 186.05, 185.58, 174.47, 162.02, 150.70, 150.67, 150.65, 149.94, 149.60, 149.47, 149.44, 149.43, 149.30, 149.12, 149.09, 148.66, 148.59, 148.41, 148.26, 148.11, 148.08, 147.80, 147.69, 147.59 (2C), 145.88, 145.69 (2C), 145.64, 145.58, 145.47 (2C), 145.22, 145.21, 145.13, 144.53, 144.46, 144.13, 142.73, 142.66, 142.31, 141.49, 141.46, 141.32, 141.06, 140.97 (2C), 140.26, 140.13, 139.53, 139.51, 136.85, 136.27, 136.15, 134.38, 133.79, 133.77, 132.94, 128.65 (2CH-aryl), 126.05 (1CH-aryl), 124.35 (2CH-aryl), 91.37 (1C, sp^3), 84.78 (1C, sp^3), 84.49 (1C, sp^3), 82.47 (1*C*$(CH_3)_3$), 81.81 (1*C*$(CH_3)_3$), 81.58 (1*C*$(CH_3)_3$), 26.92 ($3CH_3$), 26.78 ($3CH_3$), 26.69 ($3CH_3$). FT-IR (microscope): 2980, 2929, 2162, 1812, 1747, 1708, 1364, 1307, 1217, 1191, 1089, 909, 734 cm^{-1}. ESI-MS (Bruker Esquire): *m*/*z* (rel intens) 1201 (100, M + H^+).

Open-Cage Fullerene Derivate 9. To the solution of compound **6e** (30 mg, 0.025 mmol) in CH_2Cl_2 (7.5 mL) was added Br_2 (150 mg, 0.94 mmol) at room temperature. After being stirred for 5 min, the solution was washed with a $Na_2S_2O_3$ and K_2CO_3 mixed solution (300 mg of $Na_2S_2O_3$, 200 mg of K_2CO_3 dissolved in 5 mL of water). The organic layer was directly chromatographed on a silica gel column (20 × 100 mm) eluting with toluene/petroleum ether/AcOEt (10:10:1). The red band was collected and evaporated. The residue was further purified by another silica gel column (20 × 30 mm) eluting with toluene/petroleum ether (1:1) to remove some impurities. Then the eluting solvent was changed to toluene/petroleum ether/AcOEt (10:10:1). The red band was collected and evaporated to give **9** as the major product (18 mg, 0.014 mmol, 57%). Another minor isomer was also noticed but not enough for characterization. ^1H NMR (400 MHz, $CDCl_3$:CS_2 = 1:1): δ 7.82−7.80 (2H), 7.49−7.45 (2H), 7.28−7.24 (1H), 1.35 (s, 9H), 1.29 (s, 9H), 1.25 (s, 9H). ^{13}C NMR (100 MHz, $CDCl_3$:CS_2 = 1:1): all signals represent 1C except as noted (one carbonyl signal is covered by the signal of CS_2); δ 185.17, 161.98, 160.16, 150.15, 149.77, 149.70, 149.37, 149.29, 149.22, 149.13 (2C), 149.05 (2C), 148.64, 148.59, 148.52, 148.46, 148.44, 148.31, 148.18, 147.86, 147.83, 147.61, 147.34, 146.84, 146.51, 146.04, 145.87, 145.45, 145.44, 145.38, 145.37, 145.29, 145.15, 145.03 (2C), 144.60, 144.08, 143.62, 142.85, 142.24, 141.97, 141.85, 141.54, 141.49, 141.19, 140.90, 139.93, 139.50, 139.47, 138.73, 138.71, 138.27, 136.10, 133.38, 133.01, 130.95, 128.51 (2CH-aryl), 126.24 (1CH-aryl), 125.71 (2CH-aryl), 86.55 (1C, sp^3), 84.30 (1C, sp^3), 83.16 (1C, sp^3), 83.00 (1*C*$(CH_3)_3$), 81.72 (1*C*$(CH_3)_3$), 81.50 (1*C*$(CH_3)_3$), 26.91 ($3CH_3$), 26.72 ($3CH_3$), 26.60 ($3CH_3$). FT-IR (microscope): 2980, 2930, 1816, 1738, 1694, 1489, 1454, 1389, 1365, 1214, 1190, 1114, 1093, 1081, 994, 953, 911, 867, 768, 733 cm^{-1}. ESI-MS (Bruker Esquire): *m*/*z* (rel intens) 1190 (100, M − (−N═N−Br) + (−OMe) + H^+).

Open-Cage Fullerene Derivate 11. To the solution of compound **9** (51 mg, 0.040 mmol) in CH_2Cl_2 (50 mL) was added $AgClO_4$ (35 mg, 0.17 mmol) at room temperature. After being stirred for 1 h, the solution was directly chromatographed on a short column (35 × 30 mm) eluting with CH_2Cl_2/CH_3OH (4:1). The eluting solution was washed with a $NaHCO_3$ solution (30 mg of $NaHCO_3$ dissolved in 30 mL of water). The organic layer was directly chromatographed on a silica gel column (35 × 300 mm) and slowly eluted with CH_2Cl_2/CH_3OH (4:1) for about 30 min. The red band was collected and evaporated. The residue was further chromatographed on a silica gel column (20 × 30 mm) eluting with toluene/AcOEt (40:1). The red band was collected and evaporated to give **11** (29 mg, 0.027 mmol, 68%). ^1H NMR (400 MHz, $CDCl_3$:CS_2 = 1:1): δ 7.67−7.65 (2H), 7.52−7.48 (2H), 7.28−7.26 (1H), 1.29 (s, 9H), 1.24 (s, 9H). ^{13}C NMR (100 MHz, $CDCl_3$:CS_2 = 1:1): all signals represent 1C except as noted; δ 183.00, 182.74, 182.53, 161.30, 149.60, 149.52, 149.47, 149.44, 149.41, 149.34 (2C), 149.31 (2C), 148.04, 148.02, 148.01, 147.99, 147.97, 147.92 (2C), 147.30, 147.28, 147.14, 146.95, 146.79, 146.35, 145.62, 145.46, 145.35 (2C), 145.27 (2C), 145.16, 145.07, 145.03, 144.53, 144.47 (2C), 144.36, 144.31, 143.45, 143.44 (2C), 143.37, 142.05, 141.81, 141.27, 141.08, 138.80, 138.40, 137.88, 137.51, 136.11, 135.57, 134.69, 128.84, 128.80 (2CH-aryl), 128.65, 126.09 (1CH-aryl), 125.12, 124.31 (2CH-aryl), 84.30 (1C, sp^3), 83.58 (1C, sp^3), 81.91 (1*C*$(CH_3)_3$), 81.71 (1*C*$(CH_3)_3$), 26.96 ($3CH_3$), 26.73 ($3CH_3$). FT-IR (microscope): 2980, 2929, 1811, 1747, 1695, 1490, 1364, 1216, 1191, 1090, 958, 908, 732 cm^{-1}. ESI-MS (Bruker Esquire): *m*/*z* (rel intens) 1058 (100, M + H^+).

Open-Cage Fullerene Derivate 12. To the solution of compound **10** (38 mg, 0.032 mmol) in CH_2Cl_2 (38 mL) was added $AgClO_4$ (27 mg, 0.13 mmol) at room temperature. After being stirred for 1 h, the solution was directly chromatographed on a short column (35 × 30 mm) eluting with CH_2Cl_2/CH_3OH (4:1). The eluting solution was washed by $NaHCO_3$ solution (22 mg of $NaHCO_3$ dissolved in 22 mL of water). The organic layer was directly chromatographed on a silica gel column (35 × 300 mm) and slowly eluted with CH_2Cl_2/CH_3OH (4:1) for about 30 min. The red band was collected and evaporated. The residue was further eluted with toluene/AcOEt (40:1) on a silica gel column (20 × 30 mm). The red band was collected and evaporated to give **12** (22 mg, 0.022 mmol, 70%). ^1H NMR (400 MHz, $CDCl_3$:CS_2 = 1:1): δ 7.70−7.68 (2H), 7.51−7.47 (2H), 7.33−7.30 (1H), 6.77 (s, 1H), 1.21 (s, 9H). ^{13}C NMR (100 MHz, $CDCl_3$:CS_2 = 1:1): all signals represent 1C except as noted; δ 182.70, 182.14, 181.99, 159.55, 149.50, 149.33, 149.16, 149.10 (2C), 149.06 (2C), 149.02, 148.99 (2C), 148.93, 148.44, 147.95, 147.80 (2C), 147.76, 147.66, 147.62 (2C), 147.43, 147.07, 146,75, 146.60, 146.50, 145.41, 145.30, 145.25, 144.76, 144.64, 144.58, 144.40, 144.32 (2C), 144.23, 144.14, 143.85, 143.35, 143.07 (2C), 143.05 (2C), 142.46 (2C), 142.30, 141.97, 141.11, 140.51, 137.39, 137.06, 134.95, 134.42, 132.08, 129.16, 128.90 (2CH-aryl), 127.23 (1CH-aryl), 126.26, 125.43 (2CH-aryl), 83.49 (1C, sp^3), 81.71 (1*C*$(CH_3)_3$), 76.03 (1C, sp^3), 26.24 ($3CH_3$). FT-IR (microscope): 3364, 2976, 2924, 2852, 1823, 1745, 1673, 1491, 1364, 1189, 1116, 1089, 906, 733 cm^{-1}. ESI-MS (Bruker Esquire): *m*/*z* (rel intens) 1008 (100, M + Na^+).

Open-Cage Fullerene Derivate 13. To the solution of compound **12** (28 mg, 0.028 mmol) in CH_2Cl_2 (5 mL) was added Br_2 (1.3 g, 8.1 mmol) at room temperature. After being stirred for 1 h, the solution was washed with a Na_2SO_3 solution (2.5 g of Na_2SO_3 dissolved in 10 mL of water). The organic layer was evaporated. The residue was

further chromatographed on a silica gel column (20 × 50 mm) eluting with toluene/AcOEt (40:1). The first red band was collected and evaporated to give **13** (15 mg, 0.014 mmol, 50%). The second red band was collected and evaporated to give the unreacted **12** (9 mg, 0.0091 mmol, 32%). ^{1}H NMR (400 MHz, $CDCl_3$:CS_2 = 1:1): δ 7.61(s, 4H), 6.62 (s, 1H), 1.22 (s, 9H). ^{13}C NMR (100 MHz, $CDCl_3$:CS_2 = 1:1): all signals represent 1C except as noted; δ 183.28, 182.66, 182.54, 165.68, 159.68, 150.30, 149.65, 149.44 (2C), 149.39, 149.37, 149.35 (2C), 149.31, 149.28, 149.26, 148.64, 148.23, 148.08 (2C), 148.06, 147.97, 147.92 (2C), 147.73, 147.38, 147.06, 146.87, 146.76, 145.61, 145.59, 145.48, 145.06, 144.81, 144.72, 144.65, 144.58, 144.52, 144.47, 144.32, 144.05, 143.46, 143.40 (2C), 143.39, 143.37, 142.62, 142.32, 141.75, 141.43, 140.83, 137.67, 137.52, 137.34, 135.19, 134.66, 132.74, 132.36 (2CH-aryl), 129.43, 127.32 (2CH-aryl), 126.60, 121.68, 83.77 (1C, sp^3), 82.14 (1*C*$(CH_3)_3$), 76.27 (1C, sp^3), 26.57 ($3CH_3$). FT-IR (microscope): 3381, 2978, 2927, 1825, 1746, 1678, 1482, 1365, 1116, 1089, 906, 732 cm^{-1}. ESI-MS (Bruker Esquire): *m*/*z* (rel intens) 1104 (100, M + K$^+$).

Crystals suitable for X-ray diffraction were obtained from slow evaporation of **13** in a mixture of CS_2, $CHCl_3$, and $C_2H_4Cl_2$ (1:1:1). Crystal system, space group: triclinic, $P\bar{1}$. Unit cell dimensions: a = 11.6078(3) Å, α = 87.253(2)°, b = 14.2697(4) Å, β = 85.787(2)°, c = 14.6697(4) Å, γ = 88.3700(10)°, volume 2419.78(11) Å^3. Final R indices [$I > 2\sigma(I)$]: R1 = 0.0497, wR2 = 0.1108.

General Procedure for the Conversion of 6 to 7 (or 11 to 12) Using CuBr as the Reductant. To a stirred solution of compound **6a** (20 mg, 0.015 mmol) in CH_2Cl_2 (5 mL) was added anhydrous CuBr (10 mg, 0.07 mmol) at room temperature. After 1 h, the solution was directly chromatographed on a silica gel column (20 × 50 mm) eluting with toluene/petroleum ether/AcOEt (10:10:1). The red band was collected and evaporated to give **7a** (17 mg, 0.014 mmol, 90%). The yield of **12** from **11** was also 90%.

General Procedure for the Conversion of 9 to 6e (or 10 to 7e) Using $Na_2S_2O_3$ as the Reductant. To a stirred solution of compound **9** (20 mg, 0.016 mmol) in CH_2Cl_2 (5 mL) was added $Na_2S_2O_3$ (100 mg, 0.63 mmol dissolved in 1 mL of H_2O) at room temperature. After 1 min, the solution was directly chromatographed on a silica gel column (20 × 50 mm) eluting with toluene/petroleum ether/AcOEt (5:5:1). The red band was collected and evaporated to give **6e** (19 mg, 0.016 mmol, 100%). A quantitative yield was also obtained from **10** to **7e**.

Preparation of H_2O@13. To a solution of compound **13** (20 mg, 0.019 mmol) in toluene (20 mL) was added water (2 mL). After being stirred at 80 °C for 5 h, the solution was directly chromatographed on a silica gel column (20 × 30 mm) eluting with toluene/petroleum ether/AcOEt (10:10:1). The red band was collected and evaporated to give H_2O@**13** (15 mg, 0.014 mmol, 74%). ^{1}H NMR (300 MHz, $CDCl_3$): δ 7.64 (m, 4H), 6.70 (s, 0.78H), 6.68 (s, 0.22H), 1.22 (s, 9H), −13.12 (s, 1.56H). ^{13}C NMR (150 MHz, CS_2:$CDCl_3$ = 5:1): all signals represent 1C except as noted; δ182.73, 182.10, 181.86, 158.34, 150.04, 149.50, 149.29, 149.25, 149.18 (2C), 149.14, 149.09, 149.05, 148.92, 148.17, 147.80 (2C), 147.72, 147.70, 147.67, 147.52, 147.41, 147.26, 146.91, 146.86, 146.73, 145.23, 145.14, 145.08, 144.79 (2C), 144.68, 144.59, 144.46 (2C), 144.10, 144.00, 143.68, 143.28, 143.26, 143.22 (2C), 143.07, 143.02, 143.00, 142.44, 142.22, 141.47, 141.33, 140.67, 137.48, 137.31, 137.23, 134.91, 134.46, 132.40, 132.02 (2CH-aryl), 129.76, 126.92 (2CH-aryl), 126.88, 121.36, 83.46 (1C, sp^3), 81.68 (1*C*$(CH_3)_3$), 75.98 (1C, sp^3), 26.21 ($3CH_3$). FT-IR (microscope): 3413, 2984, 2256, 1811, 1743, 1677, 1483, 1188, 1118, 909, 730 cm^{-1}. ESI-MS (Bruker Esquire): *m*/*z* (rel intens) 1114 (100, M + H_2O + MeO^-).

Crystals suitable for X-ray diffraction were obtained by storing the $CDCl_3$ solution of H_2O@**13** in the NMR tube at −20 °C. Crystal system, space group: triclinic, $P\bar{1}$. Unit cell dimensions: a = 14.3254(2) Å, α = 78.9479(9)°, b = 14.6236(2) Å, β = 67.0876(9)°, c = 15.6704(3) Å, γ = 62.6231(7)°, volume 2684.79(7) Å^3. Final R indices [$I > 2\sigma(I)$]: R1 = 0.0465, wR2 = 0.1108.

Preparation of H_2O@14. To a solution of compound **1** (18 mg, 0.017 mmol) in CH_2Cl_2 (10 mL) were added ferrocene (120 mg, 0.65 mmol) and TFA (80 mg, 0.70 mmol) at 30 °C. The color of the solution was suddenly changed from light red to dark brown. After being stirred for 1 min, the solution was directly chromatographed on a silica gel column (20 × 50 mm) eluting with toluene/petroleum ether/AcOEt (5:5:1). The red band was unreacted ferrocene and a trace amount of compound **1**. Then the eluting solvent was changed to toluene/petroleum ether/AcOEt (2:2:1). The red band was collected and evaporated to give a crude product (10 mg). The crude product was further purified by another silica gel column (20 × 50 mm) eluting with toluene/AcOEt (20:1). The first dark red band was collected and evaporated to give H_2O@**14** (3 mg, 0.0033 mmol, 19%). ^{1}H NMR (600 MHz, $CDCl_3$): δ7.80−7.78 (m, 2H), 7.61−7.59(m, 2H), 7.37−7.34 (m, 1H), −12.75 (s, 1.07H). Because of the low solubility of compound **3**, the ^{13}C NMR spectrum did not give a satisfying result. FT-IR (microscope): 1800, 1738, 1689, 909, 729 cm^{-1}. ESI-MS (Bruker Esquire): *m*/*z* (rel intens): 926 (30, M + MeO^-), 958 (100, M + CH_3OH + MeO^-).

Crystals suitable for X-ray diffraction were obtained by storing the $CDCl_3$ solution of H_2O@**14** in the NMR tube at −20 °C. Crystal system, space group: triclinic, $P\bar{1}$. Unit cell dimensions: a = 12.7939(3) Å, α = 80.4622(9)°, b = 14.6804(3) Å, β = 89.7112(10)°, c = 14.8585(4) Å, γ = 69.6389(9)°, volume 2576.00(11) Å^3. Final R indices [$I > 2\sigma(I)$]: R1 = 0.0658, wR2 = 0.1863.

CCDC-626001, CCDC-600196, CCDC-652051, CCDC-658256, and CCDC-658257 contain the crystallographic data for **4l′**, **6a**, **13**, H_2O@**13**, and H_2O@**14**, respectively. The crystallographic data can be obtained free of charge via www.ccdc.cam.ac.uk/consts/retrieving-.html (or from the Cambridge Crystallographic Data Centre, 12 Union Rd., Cambridge CB12 1EZ, U.K., fax (+44)1223−366-033 or e-mail deposit@ccdc.cam.ac.uk).

Acknowledgment. Financial support is provided by NNSFC (Grants 20632010, 20521202, and 20472003), the Ministry of Education of China, and the Major State Basic Research Development Program (Grant 2006CB806201).

Supporting Information Available: Experimental procedure and characterization data for compounds not listed in the Experimental Section, crystallographic data for **4l′**, **6a**, **13**, H_2O@**13**, and H_2O@**14**, and selected NMR, MS, IR, and UV−vis spectra. This material is available free of charge via the Internet at http://pubs.acs.org

JA0763798